Program/Abstract Book

8th International Workshop on High-Resolution Depth Profiling

Western University
London, Ontario, Canada
August 7 — 11, 2016

CAP ENGINEERING
Solutions & Services

Skills & Expertise

Our knowledge is based on 20 years of experience in the field of ion implanters. Our areas of expertise revolve around this experience and the latest scientific advances in the field. Our areas of activity are diverse and remain open as needed: allowance of special mechanical, design of R & D ion implanters, ion sources, card or electronic racks design, refurbish of existing equipment, upgrading, equipment maintenance and leak detections. Because we know the problems researchers face and their constraints, we can respond best to all requests. That's why universities and research laboratories in Europe, South Africa. US and Canadian have chosen to trust us.

Research,design and manufacture

From project to design, CAP Engineering Solutions & Services follows your project and works hard to achieve it from beginning to end. All our machines are unique, manufactured according to specific requests, allowing researchers to conduct their tests as needed.

Refurbishing and upgrading

We can manufacture bespoke special machines but we also work on existing machines for refurbishing, renovating, add functionality, improve their performance. A service extremely valued by the researchers wishing to develop or simply to update the machines on which they work.

R&D ion implanters

The implanters that we design for R &D are manufactured specifically to allow the researchers to obtain equipment adapted to their research and to their objectives.

Equipment and machine maintenance

Whatever the type of machine, our team can visit for any maintenance:

- Preventive or curative maintenance
- Revisions, regulations, controls
- Audits and diagnoses
- Electronic, mechanical repairs
- Helium leak check

Our team can work on equipment manufactured by CAP Engineering Solutions & Services and also on other machines and ion implanters.

Our references :

UNIVERSITY OF THE WITWATERSRAND, JOHANNESBURG

INSA INSTITUT NATIONAL DES SCIENCES APPLIQUÉES TOULOUSE

McMaster University
Inspiring Innovation and Discovery

Phone : +33 (0) 442 650 462 Mail : info@capess.fr Web : www.capess.fr
CAP Engineering Solution & Services 602, av. des Chasséens, ZI AVON – 13120 GARDANNE – FRANCE

TABLE OF CONTENTS

Physics and Astronomy Building, First Floor Plan 2

Sponsors 3

Welcome Message from the HRDP8 Chair 5

Committees 6

Previous Meetings on HRDP 6

Important Information 7

Information for Presenters – Oral 10

Information for Session Chairs 11

Information for Presenters – Poster 11

Overview of HRDP8 12

Program at a Glance 13

Scientific Program 17

Abstracts - Oral 25

Abstracts – Poster 77

Author Index 99

CAP Engineering Solutions & Services .... Inside front cover

Systems for Research .... Inside back cover

Western University Map .... Outside back cover

Physics and Astronomy Building

First Floor

to buses

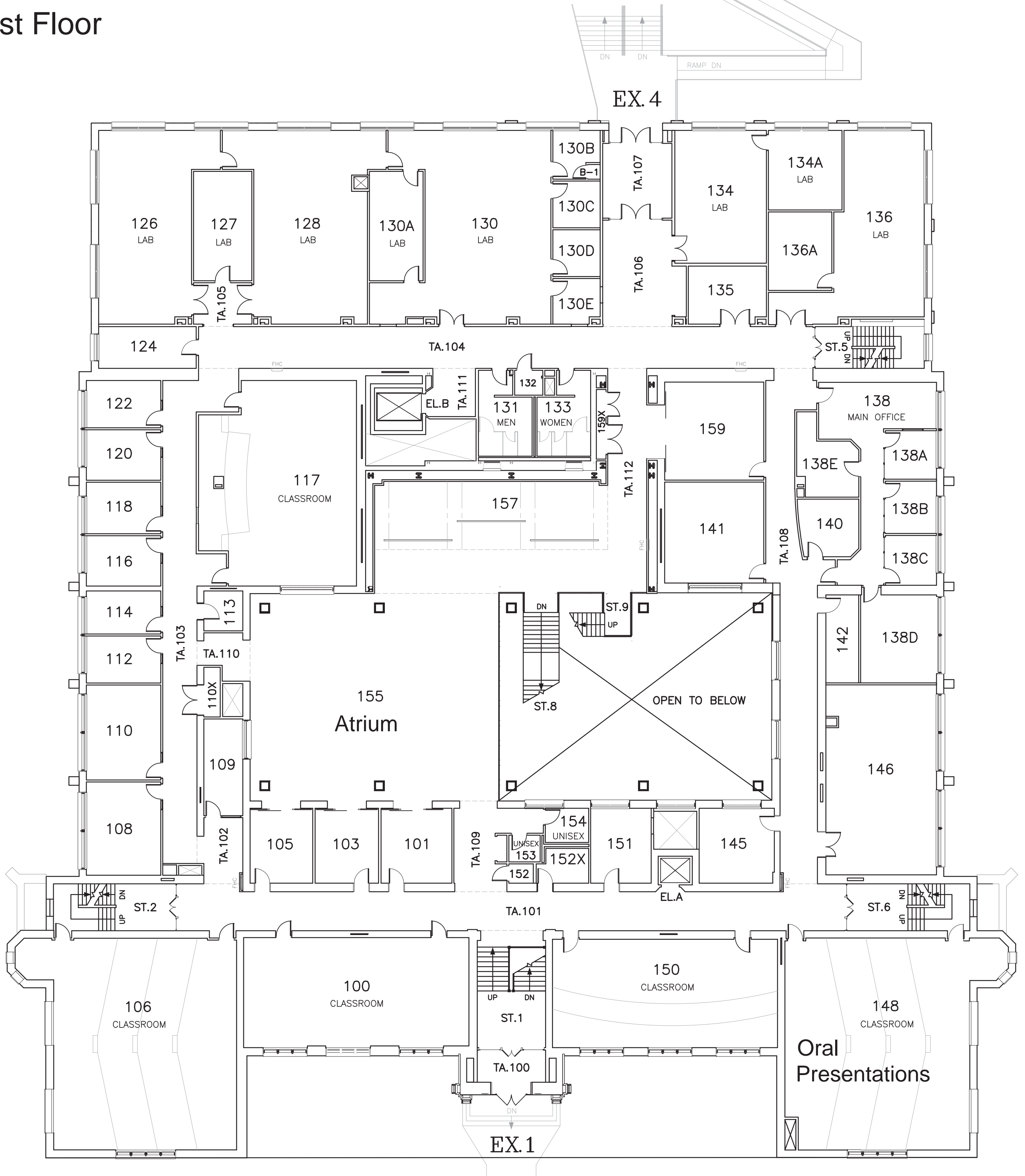

OUR SPONSORS

We are very grateful to the following sponsors without whose support the 8th International Workshop on High-Resolution Depth Profiling would not have been possible.

Department of Physics and Astronomy	http://www.physics.uwo.ca/
Tandetron Accelerator Facility	http://www.isw.physics.uwo.ca/
	http://www.highvolteng.com/
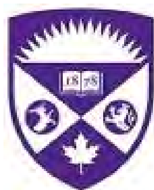 Western Science	http://www.uwo.ca/sci/

Continued on next page

http://www.surfacesciencewestern.com/

Professor Emeritus Ian Mitchell

Department of Chemistry http://www.uwo.ca/chem/

Professor Peter J. Simpson http://www.physics.uwo.ca/~psimpson/

Welcome to the 8th International Workshop on High-Resolution Depth Profiling!

On behalf of the local organizing committee, it is our pleasure to welcome you to the 8th High-Resolution Depth Profiling Workshop in London, Canada. This year's scientific sessions will cover many established ion depth profiling methods, including low and medium energy ion scattering, nuclear resonance profiling and high resolution SIMS. We have also invited experts to introduce some emerging techniques: helium ion microscopy, atom probe topography and application of neutron scattering and reflectivity for depth-profiled information.

The HRDP8 workshop will be held at Western University, one of the oldest universities in Canada, celebrating its 140th anniversary in 2018. Most of the workshop activities will take place in the recently-renovated Physics and Astronomy building, in the centre of our original, beautiful campus. The social program will include a trip to Niagara Falls, including a boat tour, followed by a banquet at the Canadian Warplane Heritage Museum. We hope there will be many great opportunities to spend enjoyable time with colleagues and have productive discussions about our challenges, new developments and opportunities.

Immediately following the workshop, there will be an HRDP tutorial day to present various techniques used in depth profiling. This tutorial is intended for a new HRDP generation, offering many students the opportunity to learn from experts in these fields. The tutorial has attracted over 13 young participants, a number of whom plan to participate at the workshop.

The workshop and tutorial have been sponsored by Western University and participating facilities and departments. We have benefitted from strong support from our industrial sponsors, whom we would like to thank.

We hope that you will enjoy the workshop and all that Western can offer!

Lyudmila Goncharova and the HRDP8 team

London, Canada, August 2016

COMMITTEES

International Scientific Committee

Paul Bailey, UK
Matt Copel, USA
Pedro Grande, Brazil
Torgny Gustafsson, USA
Yoshiaki Kido, Japan
Kenji Kimura, Japan
Takanori Koshikawa, Japan
Dae Won Moon, Korea
John O'Connor, Australia
Ian Vickridge, France
Phil Woodruff, UK

Local Organizing Committee

Lyudmila Goncharova, Chair
Giovanni Fanchini
David Shoesmith
Peter Simpson
Myra Gordon

PREVIOUS INTERNATIONAL WORKSHOPS ON HIGH-RESOLUTION DEPTH PROFILING

7th International Workshop on High Resolution Depth Profiling
July 8-11, 2013, Singapore

6th International Workshop on High-Resolution Depth Profiling
June 27 – 30, 2011, Paris, France

5th International Workshop on High-Resolution Depth Profiling
November 15-19, 2009, Kyoto, Japan

4th International Workshop on High-Resolution Depth Profiling
June 17 – 21, 2007, Radebeul, Germany

International Workshop on High Resolution Depth Profiling
May 23 – 26, 2005, Bar Harbor, Maine, USA

2nd International Workshop on Ion Beam Techniques for the Analysis of Composition and Structure with Atomic Layer Resolution
September 24–27, 2002, Kyongju, Korea

Ion Beam Techniques for the Analysis of Composition and Structure with Atomic Layer Resolution (28th IUVSTA Workshop)
June 26 - 30, 2000, Abingdon, Oxfordshire, UK

Important Information

Badges
Please wear your badge to all HRDP8-related activities.

Locations
There is an annotated campus map on the outside back cover of the Program/Abstract Book.

All oral sessions take place in room 148 in the Physics and Astronomy Building (PAB).

Coffee breaks will be held in the Atrium in the Physics and Astronomy Building.

The poster session will be held in the Atrium in the Physics and Astronomy Building.

Lunches on Monday, Tuesday and Thursday will be held in The Wave on the second floor of the University Community Centre; bag lunches may be picked up in the Atrium in the Physics and Astronomy Building on Wednesday (and on Friday for those participating in the Tutorial).

Smoking
Smoking is prohibited in all campus buildings and within 10 metres of any building entrance, loading dock or fresh air intake (including windows that open) as well as in designated "Clear Air Corridors".

If you are at a HRDP8-sponsored activity and you must smoke, please go outside; however, if you have an alcoholic beverage in your hand, ...

Alcoholic Beverages
You are now in Ontario. Regulations are strict with regard to where you may drink, even at HRDP8-sponsored functions. If you are told by someone official, including student volunteers, that you cannot bring your alcoholic beverage into the hallway, into the next room, outside, off the patio, etc., please comply.

Wildlife
The Western campus (and North London) is home to a wide variety of wildlife including Canada geese, red-tailed hawks, gulls, many species of smaller birds, squirrels, chipmunks, raccoons, skunks, woodchucks and deer. Most will not cause you any problems, however

Watch where you walk

Flocks of Canada geese are everywhere on campus; they leave a mess on sidewalks and fields.

Stay away from skunks

They are adorable nocturnal foragers, black with a white stripe down their back; they can spray a mixture of foul-smelling, irritating mercaptans a distance of three to four metres

Parking
Free parking is available in the Huron Flats lot; see the campus map on the back cover.

Copying Machines

Coin-operated copying machines can be found on various floors of the Taylor Library in the Natural Sciences Centre across the street from the Physics and Astronomy building.

Taylor Library summer hours are M – F, 08:30 – 18:00.

More complete printing/copy services are available in Books Plus across Western Road from London Hall.
Their summer hours are:
M – Th, 09:00 – 19:00; F, 09:00 – 17:00

Books Plus

In addition to providing printing/copy service, books, school and office supplies, etc., are also available in Books Plus. There is a discount coupon in your tote bag.

Western Plaza Pharmacy shares space with Books Plus. Its summer hours are:
M – Th, 09:00 – 17:00; F, 09:00 – 16:30

University Community Centre

The University Community Centre is home to many important facilities including The Wave (restaurant and pub on the second floor), where the lunches will be provided for scientific program participants on Monday, Tuesday and Thursday.

Other retail facilities in the UCC include the following:

ATMs

- Bank of Montreal, UCC main floor and UCC lower level
- CIBC, UCC lower level
- Royal Bank of Canada, UCC main floor and Natural Sciences Centre main floor
- Scotiabank, UCC lower level
- TD Canada Trust, UCC main floor

The Book Store at Western
M – F, 08:30 – 16:30 There is a discount coupon in your tote bag.

Campus Computer Store
M – F, 08:30 – 16:30

Campus Vision
M – F, 09:00 – 16:30

Creative Services
M – F, 08:30 – 16:30

The Chiropractic Clinic
M – F, mornings and afternoons, varying hours
519-661-4006

Grocery Checkout
M – Th, 10:00 – 19:30; F, 10:00 – 18:00

The Purple Store
M – F, 10:00 – 16:00

Spirit Hair Studio
M – F, 10:00 – 17:00
519-661-3087

Subway
M – F, 11:30 – 14:00

The Spoke
Café, M – F, 08:00 – 14:00
Kitchen and Bar, M – F, 11:00 – 14:00

Tim Horton's
M – Th, 07:00 – 19:30; F, 07:00 – 17:00

Tim Horton's Express
M – Th, 08:00 – 15:00, F, 08:00 – 13:00

UCC Dental
M – Th, 09:00 – 16:30; F, closed
519-850-2455

Western On-Campus Pharmacy and Canada Post
M – Th, 09:00 – 17:00; F, 09:00 – 16:30

Other Eating Places

Tim Horton's in the Natural Sciences Centre
M – F, 07:30 – 15:00

Eatery in the Ivey Business School, Richard Ivey Building
M – F, 07:30 – 14:30

Green Leaf Café in Somerville House
M – F, 11:30 – 14:00

The Grad Club

The only pub on campus open in the evening (until 23:00) is the Grad Club on the lower level of Middlesex College. Food is also served in the Grad Club.
M – F, 08:00 – 23:00

LTC Bus Pass

You may use your bus pass on any London Transit Commission bus any time, August 7 – 11; just show it to the bus driver. Some bus drivers may look at it closely to check the dates, some may ask to see your HRDP8 badge. Campus bus stops are indicated on the annotated campus map on the back cover.

INFORMATION FOR PRESENTERS – ORAL

Length of Oral Presentations

- Most contributed presentations are 25 minutes in length (check the program) including at least 5 minutes for questions; invited presentations are a total of 40 minutes in length including time for questions.

Audio-Visual Equipment

- A video-data projector and a computer with a USB port will be provided as will a VGA cable and an HDMI cable; access to the Internet is also available.
- Presenters should bring their presentation on a flash drive to the volunteer at least one-half hour before the morning or afternoon session is due to begin; they may bring it to the volunteer as early as 08:30 on Monday morning even if they will not be speaking until Thursday.
- Presenters are free to use their own laptop for their presentation but must ensure compatibility with the projector prior to the start of their session. Mac users must provide the appropriate VGA adapter.
- Connecting your own laptop to the computer will use some of the time available for your presentation; prepare accordingly.
- The computer is equipped with a DVD drive and USB port. Presenters are encouraged to bring their presentation on a USB flash drive. The computer will be running Windows 7 Enterprise with MS Office 2010 (including PowerPoint 2010) as well as Acrobat Reader.
- Please be sure to embed your fonts and graphics properly in your PowerPoint presentation. In the past, this was quite straightforward but is less so today. Please check to make sure your fonts and graphics are properly embedded and will display correctly in PowerPoint 2010 or Acrobat Reader.
- MS Media Player, VLC Media Player and Quicktime Player are installed on the computer; however, problems have occurred in the past regarding running different international editions of the software. Bringing the movie as a separate file is strongly recommended.
- Three browsers are installed, Internet Explorer, Mozilla Firefox and Google Chrome. In the event that a presenter wishes to run other software, (s)he needs to bring her/his own laptop to the presentation.
- To reiterate: Presenters are free to use their own laptop for their presentation but must ensure compatibility with the projector prior to the start of their session. Mac users must provide the appropriate VGA adapter. Connecting your own laptop to the computer will use some of the time available for your presentation; prepare accordingly.
- An overhead (transparency) projector and chalkboards are also available

INFORMATION FOR SESSION CHAIRS

- Session chairs should be present at least 10 minutes before the start of the session to meet the presenters.
- Talks are scheduled into 25- or 40-minute slots that include time for introductions and questions (and switching to a presenter's own laptop, if necessary).
- In the event of a last-minute cancellation, the timing of the other talks should not be changed. The gap should be used for a general discussion or a break.
- Preliminary comments must be completed before the first presenter's scheduled starting time.
- Session chairs should instigate and moderate questions for the presenters after their presentation as time permits.
- There will be an AV support person in the room at all times whose responsibilities include loading the presentations on the computer, operating the audiovisual equipment, adjusting lights, etc.

INFORMATION FOR PRESENTERS – POSTER

Poster Presentations

- Poster boards approximately 1.2 m high by 2.4 m wide (4' x 8') will be available on the first floor of the Atrium in the Physics and Astronomy Building. Each presenter will have the whole side but need not cover all the usable space [~1 m x ~2.1 m (~3.5' x ~7.5')].
- The location of your board space will be identified with the poster number found in the program in the Program/Abstract Book.
- Once the poster boards are in place (by noon on Monday, August 8), your poster may be installed; they **must** be installed by noon on Tuesday. They must be removed by 11:00 (end of coffee break) on Thursday but may be left up until that time for people to visit at their leisure during coffee breaks, etc.
- Appropriate materials (adhesive-backed Velcro™ dots) will be provided to allow you to attach your poster to the board; you may **not** use pins, staples, etc.
- Presenters are asked to be present during the poster session, Tuesday, 16:00 – 17:30, to answer questions by visitors (including the judges for the student poster competition) to their poster displays.
- Since a reception is being held in conjunction with the poster session, presenters should get some food and beverage at the beginning of the session.
- Posters left in the poster area after the end of HRDP8 on Thursday will be discarded.

OVERVIEW

HRDP8 will begin with registration on Sunday afternoon, August 7, 15:00 – 19:00 in London Hall; registration continues until 20:00 during the reception in London Hall which will take place between 18:30 and 21:00.

Oral sessions will begin on Monday morning and end late Thursday morning; all oral sessions will be held in the Physics and Astronomy Building, Room 148.

The poster session will be held on Tuesday afternoon in the Physics and Astronomy Building Atrium; student poster presenters may compete in a competition with cash prizes.

There will be an excursion to Niagara Falls, Ontario, including a boat tour which goes quite close to the various falls, on Wednesday afternoon, August 10 followed by a banquet (very casual dress) at the Canadian Warplane Heritage Museum in Hamilton, Ontario.

On Friday, August 12, there will be a tutorial on techniques used in high-resolution depth profiling. This tutorial is intended primarily for students but attendance is open at no additional charge to everyone registered for HRDP8 as long as you indicated your intention to attend when you registered on line.

PROGRAM AT A GLANCE

HRDP8 AT A GLANCE

	Monday, Aug. 8		Tuesday, Aug. 9		Wednesday, Aug. 10		Thursday, Aug. 11
08:00	Registration in the PAB Atrium						
		08:45	Feldman				
09:00	Welcome			09:00	Kimura	09:00	van den Berg
09:20	Bauer	09:25	Heller				
				09:40	Moon	09:40	Roth
10:00	Bruckner						
		10:05	Manichev	10:05	Schiettekatte	10:05	Vajandar
10:25	Coffee Break						
		10:30	Coffee Break	10:30	Coffee Break	10:30	Coffee Break
11:00	Copel	11:00	Primetzhofer	11:00	Moutanabbir	11:00	Baddeley
						11:25	Noël
11:40	Van den Berg	11:40	Rossall	11:40	Karner		
						11:50	Simpson
12:05	Lunch at The Wave	12:05	Lunch at The Wave	12:05	Pick up bag lunch in PAB Atrium		
						12:15	Lunch at The Wave
				12:20	Excursion to Niagara Falls		
13:30	England	13:30	Stedile				
14:10	Grande	14:10	Larochelle				
14:35	Alencar	14:35	Green				
15:00	Coffee Break	15:00	Discussion on the future of the International Workshop on HRDP				
15:30	Brocklebank						
15:55	Marmitt						
		16:00	Poster Session/ Wine and Cheese Reception in PAB Atrium		Banquet at Canadian Warplane Heritage Museum		
16:20	Moon						
17:00	Meeting of the International Scientific Committee	17:30					

All oral sessions will take place in the Physics and Astronomy Building, Room 148

All coffee breaks and the poster session/wine and cheese reception will take place in the Physics and Astronomy Atrium

SCIENTIFIC PROGRAM

SCIENTFIC PROGRAM

Sunday, August 7

15:00-20:00	Registration, London Hall
18:30-21:00	Welcome Reception, London Hall

Monday, August 8

08:00-	Registration, Physics and Astronomy Atrium
09:00-10:25	**SESSION 1, John O'Connor, Chair**
09:00-09:20	Welcoming Remarks, Physics and Astronomy Rm. 148 (all oral presentations)
09:20-10:00	01 Roth, D., Bruckner, B., Bauer, P. *Quantitative low energy ion scattering: Achievements and challenges*
10:00-10:25	02 Bruckner, B., Roth, D., Goebl, D., Juaristi, J.I., Alducin, M., Steinberger, R., Primetzhofer, D., Bauer, P. *Electronic stopping of slow protons in transition metals*
10:25-11:00	Coffee Break, Physics and Astronomy Atrium (all coffee breaks)
11:00-12:05	**SESSION 2, Giovanni Fanchini, Chair**
11:00-11:40	03 Copel, M. *MEIS of materials for post-silicon electronics*
11:40-12:05	04 van den Berg, J.A., Rossall, A.K., England, J.G., Alencar, I., Marmitt, G.G., Grande, P.L. *The characterisation of As plasma doping and processing using medium energy ion scattering*
12:05-13:30	Lunch, University Community Centre, The Wave, 2nd Floor
13:30-15:00	**SESSION 3, Matt Copel. Chair**
13:30-14:10	05 England, J.G., van den Berg, J.A., Rossall, A.K., Alencar, I., Marmitt, G.G., Trombini, H., Grande, P.L. *Combining Medium Energy Ion Scattering measurements with TRIDYN dynamic modelling to characterise a plasma doping process*

14:10-14:35	06	Avila, T.S., Fichtner, P.R.P., Hentz, A., Grande, P.L. *On the use of MEIS cartography for the determination of $Si_{1-x}Ge_x$ thin-film strain*
14:35-15:00	07	Alencar, I., Marmitt, G.G., Grande, P.L., England, J.G., Rossall, A.K., van den Berg, J.A. *Compositional depth profile investigation of plasma doped Si/SiO_2:As by Medium-Energy Ion Scattering*
15:00-15:30	Coffee Break	
15:30-17:00	**SESSION 4, Pedro Grande, Chair**	
15:30-15:55	08	Brocklebank, M., Noël, J.J., Goncharova, L.V. *Passive TiO_2 growth studies using Medium Energy Ion Scattering and Nuclear Reaction Profiling*
15:55-16:20	09	Marmitt, G.G., Nandi, S.K., Venkatachalam, D.K., Elliman, R.G., Vos, M., Grande, P.L. *Application of ERBS analysis on O diffusion in TiO_2 films*
16:20-17:00	10	Moon, D.W., Grande, P.L., Marmitt, G.G., RRT participants *International RRT of MEIS analysis of HfO_2 thin films and multiple delta layers*
17:00-	Meeting of the International Scientific Committee	

Tuesday, August 9

08:45-10:30	**SESSION 5, Torgny Gustafsson, Chair**	
08:45-09:25	11	Feldman, L.C., Gustafsson, T., Manichev, V., Wang, H. *He Ion Microscopes: Potential and pitfalls*
09:25-10:05	12	Klingner, N., Heller, R., Hlawacek, G., Gnauck, P., Facsko, S., Borany, J.v. *Ion beam analysis in a Helium Ion Microscope – elemental mapping on the nm scale*
10:05-10:30	13	Manichev, V., Garfunkel, E., Yang, J., Chhowalla, M., Lagos, M., Batson, P., Feldman, L.C., Gustafsson, T. *Helium Ion Microscopy studies of biological/biomedical samples, atomic size defects and elemental identification*
10:30-11:00	Coffee Break	

11:00-12:05 **SESSION 6, DaeWon Moon, Chair**

11:00-11:40 — 14 — Primetzhofer, D.
Electronic interactions of medium-energy ions with solids: some recent results and their implications for high-resolution depth profiling

11:40-12:05 — 15 — Noakes, T.C.Q., Mistry, S., Cropper, M.D., **Rossall, A.K.**, van den Berg, J.A.
MEIS studies of oxygen plasma cleaning of copper for fast response time photocathodes used in accelerator applications

12:05-13:30 — Lunch, University Community Centre, The Wave, 2nd Floor

13:30-16:00 **SESSION 7, Lyudmila Goncharova, Chair**

13:30-14:10 — 16 — Stedile, F.C., Pitthan, E., Corrêa, S.A., Soares, G.V., Radtke, C.
Nuclear Reaction Profiling unraveling the incorporation of water in SiO_2/SiC structures

14:10-14:35 — 17 — **Larochelle, J.-S.**, Désilets-Benoit, A., Martel, E., Borduas, G., Roorda, S.
Detection of hydrogen in steel with an N-15 nuclear resonance

14:35-15:00 — 18 — Green, R.J., Macke, S., Sawatzky, G.A.
Element, valence and orbital depth profiling with resonant x-ray reflectometry

15:00-16:00 — Discussion on the future of the International Workshop on High-Resolution Depth Profiling

16:00-17:30 **Poster Session/Wine and Cheese Reception, Physics and Astronomy Atrium**

Student Poster Competition cash prizes provided by a generous donation from Professor Emeritus Ian Mitchell, Department of Physics and Astronomy

P-1 — **Brocklebank, M.**, Goncharova, L.V., Barchet, D., Kherani, N.P.
Medium energy ion scattering and elastic recoil detection for solar silicon devices

P-2 — Cadogan, C.C., Karner, V.L., Tavares, A., Pywowarzcuk, A., Simpson, P.J., Goncharova, L.V.
Synthesis and characterisation of silicon nanoclusters in alumina

P-3 — Gaudet, J.M., Simpson, P.J.
Depth profiling of silicon quantum dots formed in ion-implanted thermal oxide thin film

P-4 — Lagutin, A.
Device for the transformation of charged particle beams using glass capillaries

P-5 Marmitt, G.G., Trombini, H., Sulzbach, M.C., Alencar, I., Grande, P.L.
PowerMEIS: RBS/MEIS simulations using cloud computing

P-6 Martínez-Flores, C., Trujillo-López, L.N., Serkovic-Loli, L.N., Cabrera-Trujillo, R.
Universal scaling of the electronic stopping cross section for swift heavy projectiles colliding with atoms and molecules

P-7 Min, W.J., Kim, W.S., Park, K., Jung, K.H., An, S.Y., Kim, J.-s., Kim, S.G., Sim, C.S., Kim, S., Kim, J., Yu, K.-S., Sortica, M.A., Grande, P.L., Moon, D.W.
MEIS-K120 using 100 keV He^+ and TOF analyzer

P-8 Rideout, J., Knights, A.P., Simpson, P.J., Mascher, P., England, J.G.
Positron Annihilation Spectroscopy with in situ *ion implantation to investigate defects in semiconductors over a wide temperature range*

P-9 Zolnai, Z., Petrik, P., Deák, A., Pothorszky, S., Zámbó, D., Vértesy, G., Nagy, N., Rossall, A.K., van den Berg, J.A.
A three-dimensional analysis of Au-silica core-shell nanoparticles using medium energy ion scattering

P-10 Sortica, M.A., Grande, P.L., Radtke, C., Almeida, L.G., Debastiani, R., Dias, J.F., Hentz, A.
Structural characterization of CdSe/ZnS quantum dots using Medium Energy Ion Scattering

P-11 Sulzbach, M.C., Marmitt, G.G., Pereira, L.G., Grande, P.L.
Characterization of resistive memories using micro-beam RBS

P-12 Trombini, H., Marmitt, G.G., Alencar, I., Hatori, M., Grande, P.L., Dias, J.F., Assmann, W., Toulemonde, M., Trautman, C.
Characterization of ejected CaF_2 by swift heavy ion bombardment using MEIS

P-13 Trombini, H., Marmitt, G.G., Grande, P.L., Alencar, I., England, J.G.
3D characterization of nanostructures using MEIS

P-14 Zalm, P.C., Bailey, P., Rossall, A.K., van den Berg, J.A.
Quantitative considerations in medium energy ion scattering analysis of nanolayers

P-15 Xiao, Q.F., Cui, X.Y., Hu, Y.F., Sham, T.K.
Bulk-sensitive Hard X-ray Photoelectron Spectroscopy facility at Canadian Light Source

Wednesday, August 10

09:00-10:30	SESSION 8, Jaap van den Berg, Chair		
09:00-09:40		19	Nakajima, K., Nagano, K., Marumo, T., Yamamoto, K., Narumi, K., Saitoh, Y., Hirata, K., Kimura, K. *Transmission SIMS: A novel approach to achieving higher secondary ion yields of intact biomolecules*
09:40-10:05		20	Kim, H.J., Chung, K.W., Moon, D.W. *Investigation of electric double layer at liquid interface with TOF-MEIS*
10:05-10:30		21	Schiettekatte, F. *Multiple scattering and geometry effects on depth profiling of 2D and 3D structures*
10:30-11:00	Coffee Break		
11:00-12:05	SESSION 9, Daniel Primetzhofer, Chair		
11:00-11:40		22	Moutanabbir, O. *3-D atom-by-atom dissection of materials*
11:40-12:05		23	**Karner, V.L.**, McFadden, R.M.L., Chatzichristos, A., Fujimoto, D., McKenzie, I., Morris, G.D., Cortie, D.L., Kiefl, R.F., MacFarlane, W.A. *Beta-detected Nuclear Magnetic Resonance (β-NMR): Towards depth resolved NMR*
12:05-12:20	Pick up bag lunch, Physics and Astronomy Atrium		
12:20-24:00	Excursion to Niagara Falls, Banquet at Canadian Warplane Heritage Museum		

Thursday, August 11

09:00-10:30	SESSION 10, Kenji Kimura, Chair		
09:00-09:40		24	van den Berg, J.A., Rossall, A.K., Bailey, P., Barlow, R.J. *MEIS regained at the IIAA in Huddersfield University*
09:40-10:05		25	Roth, D., Bruckner, B., Mardare, A., McGahan, Ch.L., Dosmailov, M., Juaristi, J.I., Alducin, M., Primetzhofer, D., Haglund, Jr., R.F., Pedarnig, J.D., Bauer, P. *Electronic stopping of slow protons in oxides*
10:05-10:30		26	**Vajandar, S.K.**, Wang, W., Chan, T.K., Tok, E.S., Yeo, Y.C., Osipowicz, T. *Interface strain study of ultra-thin HfO_2 films on Ge and GeSn substrates using HR-RBS*

10:30-11:00	Coffee Break

11:00-12:15 SESSION 11, René Heller, Chair

11:00-11:25 27 Murdoch, A., Trant, A.G., Gustafson, J., Jones, T.E., Noakes, T.C.Q., Bailey, P., Baddeley, C.J.
A MEIS, STM and RAIRS investigation of the adsorption of CO on cobalt/palladium bimetallic surfaces

11:25-11:50 28 Noël, J.J., Tun, Z., Shoesmith, D.W.
Neutron reflectometry as in situ *probe of thin film composition and layer structure for investigating corrosion and hydrogen absorption in titanium*

11:50-12:15 29 Simpson. P.J., Rideout, J., Knights, A.P.
Vacancy-impurity interactions in ion-implanted silicon

12:15-	Lunch, University Community Centre, The Wave, 2nd Floor

ABSTRACTS

ORAL

01

Quantitative low energy ion scattering: Achievements and challenges

D. Roth, B. Bruckner and **P. Bauer**

peter.bauer@jku.at

Johannes Kepler University Linz, Atomic Physics and Surface Science, Linz, Austria

Since its beginning some fifty years ago, Low Energy Ion Scattering (LEIS) developed to a widely used tool for analysis of structure and composition of solid surfaces, see, e.g., [1-5]. Two features contribute to the success of LEIS: first, its superb surface sensitivity and second, the fact that for most applications the yield of ions backscattered from one atomic species is independent of the other atoms present in the surface ("*absence of matrix effects",* [5-7]).

Quantitative surface composition analysis is based on accurate knowledge of the *fraction of ions* amongst the backscattered particles, P^+, and the *differential scattering cross section,* $d\sigma/d\Omega$. For that, the influence of electronic screening on nuclear scattering must be modelled precisely; the *universal potential* has been shown to be a good choice as long as not too low ion energies and too large impact parameters are employed [8]. To apprehend why in general LEIS is not sensitive to band structure effects requires understanding of the prevailing charge exchange processes – mainly *Auger neutralization* along the trajectory and *resonant charge exchange (neutralization or reionization)* in a collision [5]. Recently, it has been demonstrated that due to distinct neutralization efficiencies of different allotropic forms of carbon [9] the concentration of organic carbon on graphene can be quantified [10].

Very recently, interesting LEIS applications to ultrathin subsurface layers were reported. To gain quantitative information in this case one has to successfully handle additional processes: electronic stopping and processes related to multiple scattering: depth-dependent angular spread, increase in path length, and the loss of the unique relationship between final energy and scattering depth for a specific collision partner. To achieve quantification nevertheless, MC-simulations are required.

It will be summarized how quantitative information on P^+ can be obtained, how quantification of surface composition can be achieved, and which questions are still open [11, 12].

[1] V. Walther and H. Hintenberger, Z. Naturforschg. 18a, 843 – 853 (1963).
[2] S. Datz and C. Snoek, Phys. Rev. 134, A347 – A355 (1964).
[3] D.P. Smith, J. Appl. Phys. 38, 340 – 347 (1967).
[4] J. O'Connor in *Surface and Interface Science*, vol. 1, 269 – 310, Wiley VCH (2012), ed. K. Wandelt.
[5] H.H. Brongersma et al., Surface Science Reports 62, 63 – 109 (2007).
[6] H.H. Brongersma and P.M.Mul, Chem. Phys. Lett. 14, 380 – 384 (1972).
[7] W. Heiland and E.Taglauer, J. Vac. Sci. Techn. 9, 620 – 623 (1972).

[8] D. Primetzhofer et al., Nucl. Instr.Meth. 269, 1292 – 1295 (2011).
[9] S.N. Mikhailov et al., Nucl. Instr. Meth. B93, 210 – 214 (1994).
[10] S. Prusa et al., Langmuir 31, 9628 – 9635 (2015).
[11] P. Bruner et al., J. Vac. Sci. Techn. A33, 01A122-1 – 01A122-7 (2015).
[12] D. Goebl et al., Nucl. Instr. Meth. B354, 3 – 8 (2015).

02

Electronic stopping of slow protons in transition metals

B. Bruckner[1], D. Roth[1], D. Goebl[1], J.I. Juaristi[2,3,4], M. Alducin[2,3], R. Steinberger[5], D. Primetzhofer[6] and P. Bauer[1,3]

barbara.bruckner@jku.at

[1]Institut für Experimentalphysik, Johannes-Kepler Universität Linz, Altenbergerstraße 69, A-4040 Linz, Austria
[2]Centro de Física de Materiales CFM/MPC (CSIC-UPV/EHU), P. Manuel de Lardizabal 5, 20018 Donostia-San Sebastián, Spain
[3]Donostia International Physics Center DIPC, P. Manuel de Lardizabal 4, 20018 San Sebastián, Spain
[4]Departamento de Física de Materiales, Facultad de Químicas, Universidad del País Vasco (UPV/EHU), Apartado 1072, 20080 San Sebastián, Spain
[5]Zentrum für Oberflächen- und Nanoanalytik, Johannes-Kepler Universität Linz, Altenbergerstraße 69, A-4040 Linz Austria
[6]Institutionen för Fysik och Astronomi, Uppsala Universitet, Box 516, S-751 20 Uppsala, Sweden

When an ion propagates in matter, it loses energy due to interaction with nuclei and electrons of the target – also called nuclear and electronic stopping, respectively. The mean energy loss per path length is given by the stopping power $S = dE/dx$. Alternatively, the electronic stopping cross section ε (SCS) is defined as

$$\varepsilon = \frac{1}{n}\frac{dE}{dx},$$

where n is the atomic density of the target. Electronic stopping is well understood for large ion velocities. For slow ions, electronic stopping of a point charge in a free electron gas (FEG) is known to be proportional to ion velocity, $S \propto v$, [1 - 3]. This also holds for a FEG-metal like Al [4], as long as v is smaller than the Fermi velocity of the target electrons.

Results for noble metals show a deviation from this velocity proportionality at $v \sim 0.2$ a.u.: for gold with an excitation threshold of the d-electrons of $\sim$ 2 eV, at $v < 0.2$ a.u. the electronic SCS is dominated by the excitation of 6*s*-electrons, while for $v > 0.2$ a.u. also the *d*-band contributes [5 - 7].

For transition metals the *d*-band exhibits a high density of states (DOS) at the Fermi level, E_F, which is the basis of their high chemical reactivity. Consequently, it is demanding to produce high purity samples for electronic stopping measurements of slow ions and to minimize the influence of possible surface oxide layers and bulk impurities like hydrogen, which would impede precise measurements of electronic stopping powers in these materials.

In this contribution the low velocity electronic SCS for H^+ ions in Ni and Ta are presented. While Ni features a filled d-band with high DOS(E_F), but very low DOS($E > E_F$), the d-band of Ta is only partly filled with high DOS below and above E_F. For Ni the energy loss data were obtained from energy spectra of hydrogen ions backscattered from a high purity sheet and from nanometer Ni films of various thicknesses, prepared in-situ. Since target composition is a critical point, the samples have been analysed by x-ray induced photoelectron spectroscopy (XPS), Auger electron spectroscopy (AES) and elastic recoil detection (ERD).

The SCS of Ni and Ta are compared to data of Au [6] and Pt [8]. As can be seen in Fig. 1, at v > 0.2 a.u. (1 keV protons), Ni exhibits the lowest and Ta the highest electronic SCS, although the integrated DOS of Ni and Ta yield 11 and 5 electrons per atom, respectively. While for Ni and Pt, the experimental SCS data can be quantitatively described in terms of a FEG model, this does not hold for Ta, for which an absurdly high number of conduction electrons would be required to explain the highly efficient electronic stopping. We trace this observation back to the fact, that only Ta features high DOS both, below and above E_F so that excitation across E_F can take place with high probability. Further experiments are needed to confirm this thesis.

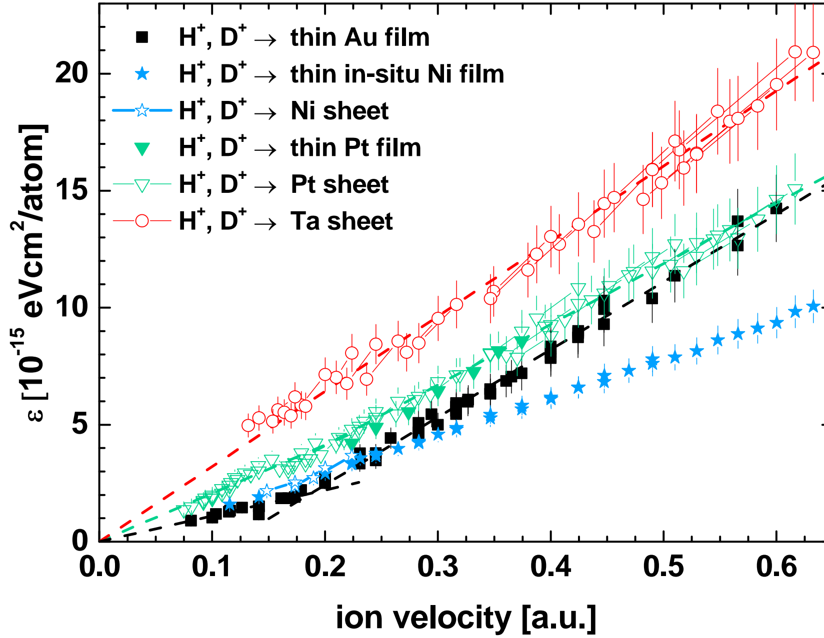

Fig. 1: Electronic stopping cross section ε of H^+ ions in Au [6], Pt [8], Ni and Ta as a function of the primary ion velocity.

References:

[1] E. Fermi, and E. Teller, *Phys. Rev.* **72**, 399 (1947)
[2] R.H. Ritchie, *Phys. Rev.* **114**, 644 (1959).
[3] P.M. Echenique, R.M. Nieminen, J.C: Ashley, and R.H. Ritchie. *Phys. Rev. A* **33**, 897 (1986).
[4] D. Primetzhofer, S. Rund, D. Roth, D. Goebl and P. Bauer, *Phys. Rev. Lett.* **107**, 163201 (2011).
[5] J.E. Valdés, J.C. Eckardt, G.H. Lantschner and N.R. Arista, *Phys. Rev. A* **49**, 1083 (1994).
[6] S.N. Markin, D. Primetzhofer, S. Prusa, M. Brunmayr, G. Kowarik, F. Aumayr and P. Bauer, *Phys. Rev. B* **78**, 195122 (2008).
[7] M.A. Zeb, J. Kohanoff, D. Sánchez-Portal, A. Arnau, J.I. Juaristi and E. Artacho, *Phys. Rev. Lett.* **108**, 225504 (2012).
[8] D. Goebl, D. Roth, and P. Bauer, *Phys. Rev. A* **87**, 062903 (2013).

MEIS of materials for post-silicon electronics

M. Copel

mcopel@us.ibm.com

IBM Research Division, TJ Watson Research Center
PO Box 218, Yorktown Hts, NY 10598 USA

The search for new devices to replace conventional silicon CMOS has stimulated research into a wide assortment of materials and architectures. The more conservative approach is to look for higher performing alternative semiconductors to replace the silicon channel. Carbon-based devices fall into this category, where a new gate stack is envisioned, but the transistor will still function as a CMOS device, with familiar logic gates. The effort to create post-CMOS devices is a more radical and ambitious program. In the post-CMOS world, new types of mechanisms are invoked to compute, and the Von Neumann architecture becomes optional. In all of these efforts, mastery of a new set of materials is crucial to success, and characterization is a valuable tool for progress.

In the realm of carbon-based electronics, medium energy ion scattering has been applied to understanding growth of multi-layer graphene. Although this has traditionally been the domain of imaging techniques, there are distinct advantages to depth-resolving methods when coupled with isotopic analysis. By using a ^{13}carbon gas precursor, we can distinguish carbon that derives from decomposition of the SiC substrate from carbon that derives from the gas phase, allowing a detailed picture of the growth mode [1]. A sample spectrum, shown below, illustrates the ability to clearly resolve carbon isotopes in multilayer graphene.

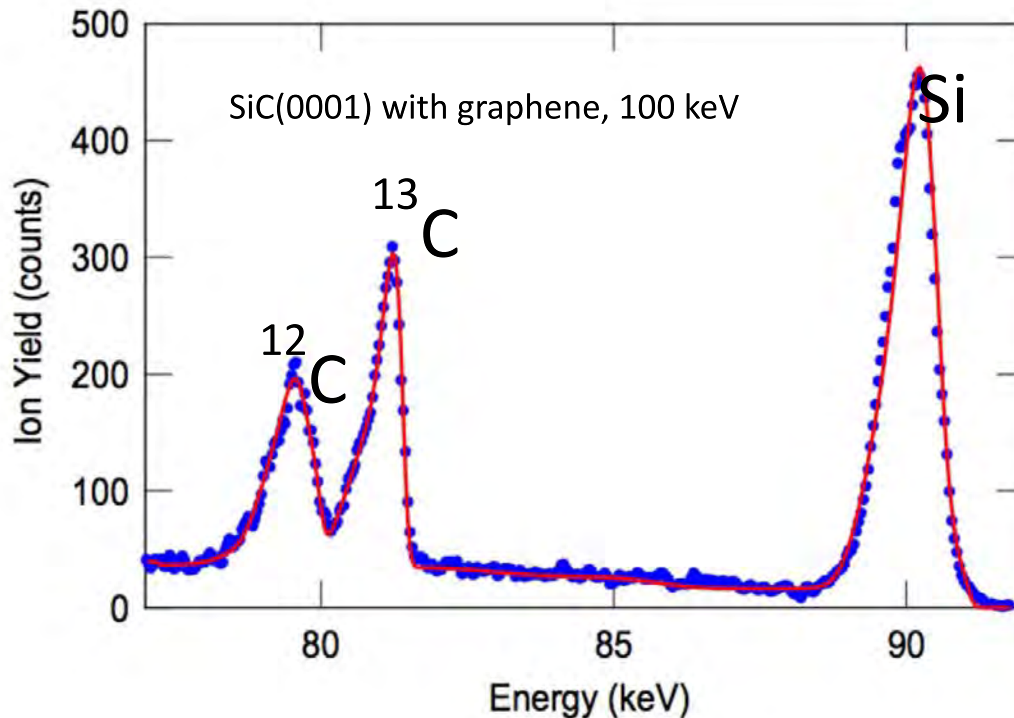

Although graphene is an attractive system for the study of two-dimensional phenomena, the lack of a conventional band gap makes it ill-suited for a logic technology. From this perspective, carbon nanotubes (CNTs) are more likely to succeed. One of the difficulties in creating a CNT logic technology is contacting the devices. For p-type devices, a high work function contact is needed. Reasonably stable metallurgies have been demonstrated, using metals such as Pd. However, for CMOS, we need n-type devices as well. This entails the use of low work function materials, whose instability causes tremendous practical problems.

A good example of a low work function contact is scandium. In a device, it would typically be deposited on a CNT lying on an insulator, such as HfO2. So the Sc must be stable in contact with HfO2, as well as any encapsulation. Yet when we deposit Sc/HfO2, we find oxygen uptake in the Sc after moderate heating. In the spectrum below, the Sc contact layer contains roughly 50% oxygen, despite processing within UHV. Some of the oxygen comes from the ambient, but much of it comes from the HfO2. (XPS confirms partial reduction of the HfO2.) Thus, the contact oxidation has the potential to both insert a series resistor in the device, and create a short circuit to the substrate.

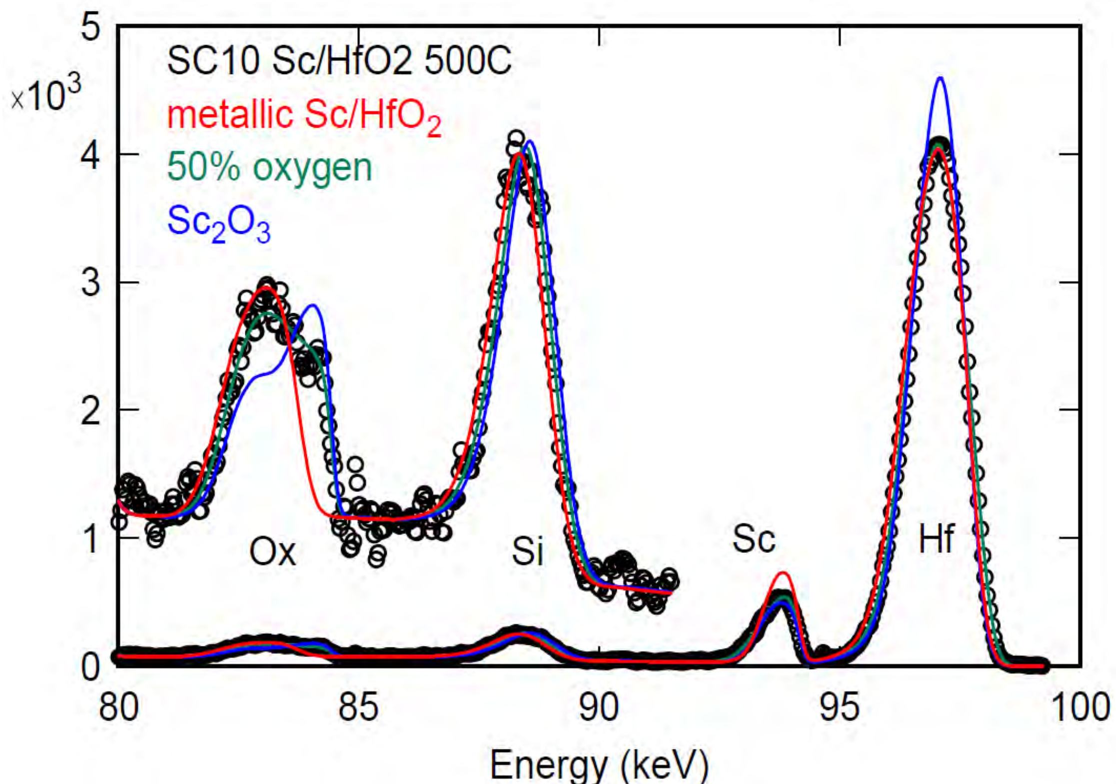

Although CNT transistors have enormous potential to extend technology, they do not qualify as post-CMOS devices. To move beyond CMOS, a radical change is needed in device concept. The PiezoElectric Transistor (PET) offers an opportunity to look at an altogether different idea [2, 3]. In the PET, a piezoelectric is used to exert pressure on a piezoresistive layer, creating a conductive path for current flow. The PET works as a

solid-state relay, using the voltage across the piezoelectric to gate the device. The PET has been the subject of a multi-year project at IBM and Penn State University, resulting in the fabrication of prototypes demonstrating resistance modulation in micron-scale devices.

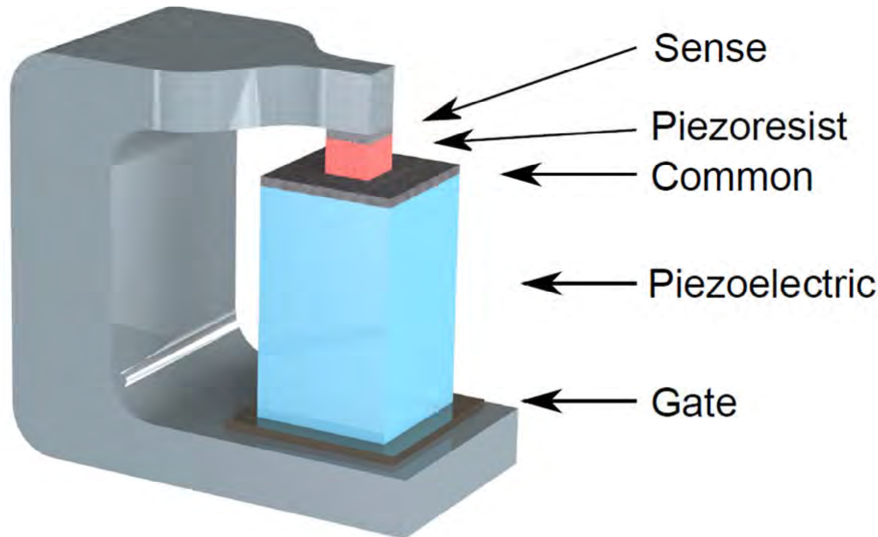

Much of the materials work in creating the PET has focused on the creation of a high-response piezoresistive layer of samarium monoselenide. Some of the challenges we encountered involved composition and stability of the piezoresist. SmSe composition is critical, since only the monochalcogenide phase exhibits piezoresistance, stable compounds exist over a wide range of selenium content. In addition, rare-earth chalcogenides need careful handling, with vulnerabilities to oxidation a source of concern. MEIS was used as a primary tool for addressing these difficulties. I will discuss some of the learning we obtained, and prospects for future development.

References.

[1] Direct Measurement of the Growth Mode of Graphene on SiC(0001) and SiC(000-1), J. B. Hannon, M. Copel, R. M. Tromp, Phys. Rev. Lett. 107, 166101 (2011).
[2] Giant piezoresistive On/Off ratios in rare-earth chalcogenide thin films enabling nanomechanical switching, M. Copel et al., Nano Letters 13, 4650 (2013).
[3] Pathway to the PiezoElectronic Transduction Logic Device, P. Solomon et al, Nano Letters 15, 2391 (2015).

The characterisation of As plasma doping and processing using medium energy ion scattering

J.A.van den Berg[1], A.K. Rossall[1], J.G. England[2], I. Alencar[3], G.G. Marmitt[3] and P.L. Grande[3]

j.vandenberg@hud.ac.uk

[1]International Institute for Accelerator Applications (IIAA), School of Computing and Engineering, University of Huddersfield, Huddersfield, HD1 3DH, UK
[21] Varian Semiconductor Equipment, Silicon Systems Group, Applied Materials Inc, 35 Dory Road, Gloucester, MA01930, USA
[3]Instituto de Física, Universidade Federal do Rio Grande do Sul, Porto Alegre, Brazil

Plasma doping (PLAD) is capable of implanting micro-electronic devices with high fluences of low energy As with high throughput. In a PLAD process considered here, a wafer was immersed in a mixed AsH_3/H_2 plasma and biased with -7 kV to effect deposition and (recoil) implantation of As from the plasma boundary into the wafer. A total ion fluence of $1\text{x}10^{16}$ cm^{-2} was measured during the implant.

MEIS analysis, using 100 keV He ions scattered through 90° in conjunction with energy spectrum simulation, was used to understand the details of this PLAD process together with the changes resulting from a subsequently applied chemical wet clean and a 1000 °C spike anneal. Although information on layer thicknesses and concentrations was sought, MEIS strictly measured areal atomic densities and information on the layer thickness was based on knowledge, or reasonable assumptions, regarding the layer density or on additional XTEM measurements.

In agreement with XTEM energy dispersive spectrometry measurements, MEIS showed that the PLAD implant process produced an intermixed As/Si layer whose As concentration decayed from a surface concentration of $\sim 2\text{x}10^{22}$ cm^{-3} to close to zero at a depth of ~20 nm, commensurate the maximum range of As ions implanted into the changing matrix. The deposited layer was capped by a 1-2 nm thin silicon oxide layer. Over a timescale of several months, As was lost by sublimation and the silicon oxide cap thickness increased.

Deposited As was removed by a wet chemical clean which, due to the presence of an oxidising agent, oxidised the Si left behind, producing a ~15nm thick Si oxide. MEIS depth profiling showed that the post clean As distribution matched the tail end of the original (recoil) implanted profile. A second sample that had undergone a similar PLAD implant but different clean showed an altered oxide thickness, and the MEIS measurements indicated where the processes differed. A detailed comparison of aligned and random MEIS spectra after annealing enabled the interstitial and substitutional As profiles to be determined. They showed that during solid phase epitaxial regrowth

of the disordered Si upon annealing, As partly moved into substitutional sites (with a concentration that correlated closely with sheet resistance measurements) whilst ~$5x10^{14}$ cm^{-2} of segregated As was trapped under the surface oxide.

Combining Medium Energy Ion Scattering measurements with TRIDYN dynamic modelling to characterise a plasma doping process

J.G. England[1], J.A. van den Berg[2], A.K. Rossall[2], I. Alencar[3], G.G. Marmitt[3], H. Trombini[3], P.L.Grande[3]

jonathan_england@amat.com

[1] Varian Semiconductor Equipment, Silicon Systems Group, Applied Materials Inc,

35 Dory Road, Gloucester, MA 01930 USA

[2] International Institute for Accelerator Applications, School of Computing and Engineering, University of Huddersfield, Huddersfield, HD1 3DH, UK.

[3] Instituto de Fısica, Universidade Federal do Rio Grande do Sul, Av. Bento Goncalves 9500, CP 15051 Porto Alegre-RS, Brazil

MEIS (Medium Energy Ion Scattering) analysis has the great advantage over other profiling methods such as SIMS and dynamic XPS and in that it can measure the absolute number of atoms in a sample without the complications of sputtering and matrix dependent effects, which are particularly important in shallow samples. Profiling by TEM/EDS does not suffer from these effects, but can only quantify profiles as atomic fractions. MEIS spectra can be transformed into depth profiles in terms of layers containing a number of atoms per unit area; converting such data to report layers of different thicknesses and atomic concentrations requires knowledge of the local density in each layer which is information strictly not contained in a straightforward MEIS energy spectrum.

Plasma doping ion implantation (PLAD) is important to enable the processing of advanced semiconductor device structures and is simple in concept: a negatively biased substrate is immersed in a plasma and doped by ions and neutrals from that plasma. The fundamental understanding of PLAD is complicated because implantation, deposition, sputtering and ion beam mixing all have to be taken into account and then additional passivation, cleaning and annealing steps have to be considered. A model of PLAD processes into planar substrates has been constructed that uses the computer code TRIDYN [1] to calculate collision cascades and hence substrate compositional changes during implantation. Rules have been proposed for how the post implant profiles are modified in the passivation and cleaning steps based on TEM/EDS measurements. A particular model prediction is that PLAD should produce a surface layer of low, graded density.

To characterise a PLAD process, several wafers were implanted with As and measured by MEIS at Huddersfield, using He at 100 keV, and at UFRGS, with H and H_2 beams at 200 keV/amu. The As, Si and O profiles for each sample were extracted from the MEIS spectra using IGOR [2] and POWERMEIS [3] based spectrum simulations. The profiles were compared for consistency with

the TRIDYN based model and were converted to atoms/cm^3 vs depth using TRIDYN model density predictions. This comparison showed that the TRIDYN based model gave a reasonable representation of PLAD but could be improved. It also suggested at which step an observed process variation had occurred. This fundamental understanding of PLAD was only possible using absolute elemental profiles measured by MEIS in combination with the TRIDYN based model.

References

[1] W. Moeller and W. Eckstein, Nucl. Instr. And Meth. B2 (1984) 814

[2] M A Reading, J A van den Berg, P C Zalm, D G Armour, P Bailey ,T C Q Noakes. A Parisini, T Conard and S De Gendt, J. Vac. Sci. Technol. B 28 (1) C65-70 (2010)

[3] Sortica et al., J. Appl. Phys. 106 (2009) 114320

06

On the use of MEIS cartography for the determination of $Si_{1-x}Ge_x$ thin-film strain

T.S. Avila, P.F.P. Fichtner, A. Hentz and **P.L. Grande**

grande@if.ufrgs.br

Implantation Laboratory, Institute of Physics, Federal University of Rio Grande do Sul, Av. Bento Gonçalves 9500, Porto Alegre, RS, Brazil

The characterization of the nanoscopic state of strain in crystalline semiconductors is important for distinct applications including, for example, the formation of extended defects, the orientation of second phase nano objects or the modification of the valence and conduction band structures and consequently the carrier mobility in semiconducting devices. In particular, strained $Si_{1-x}Ge_x$ alloys have been actively investigated during the last years because of their application in high-mobility metal-oxide-semiconductor field-effect transistors. The strain appears as a modification in atomic positions. X-ray or electron diffraction have been used to determine changes of the lattice parameter with great.

As distinct from diffraction and phase contrast techniques, H and He ion scattering techniques have been extensively employed to determine strain because changes in the channeling or blocking directions can be easily related to lattice deformations. Recently medium-energy ion scattering (MEIS) has been successfully used to determine the depth strain profile in thin Si overlayers on SiGe heterostructures [1], quantum dots [2], and nanowires [3] among other applications. Another powerful ion-beam technique namely High Resolution Rutherford Backscattering Spectrometry (HRRBS), which is comparable to MEIS, has been applied recently to get the strain profile across the HfO_2 /Si(001) [4]. Most of these methods are based on the determination of the shift in the backscattering yield minima around a given main crystallographic direction using a one-dimensional angular scan. The use of a two-dimensional yield mapping is less frequent but improves the strain measurement.

Recently, Jalabert [5] has proposed a new method to evaluate the strain state of a target material called MEIS cartography. In this method the stereographic projection of a single crystal can be measured with a standard MEIS technique for a selected atomic element and depth. Here we demonstrate that this technique can be expanded to characterize strained SiGe heterostructures with high accuracy. In this method, not only the main crystalline directions are analyzed but also the higher index ones. The advantage of this method is its elemental sensitivity with depth resolution and its capability to be used in nano-structured materials. The determination of the strain is based on the position of the many blocking lines contrary to the traditional methods where two directions are used. We also provide a method to determine the lattice deformation fitting the data best and checked it against full Monte-Carlo simulations [6].

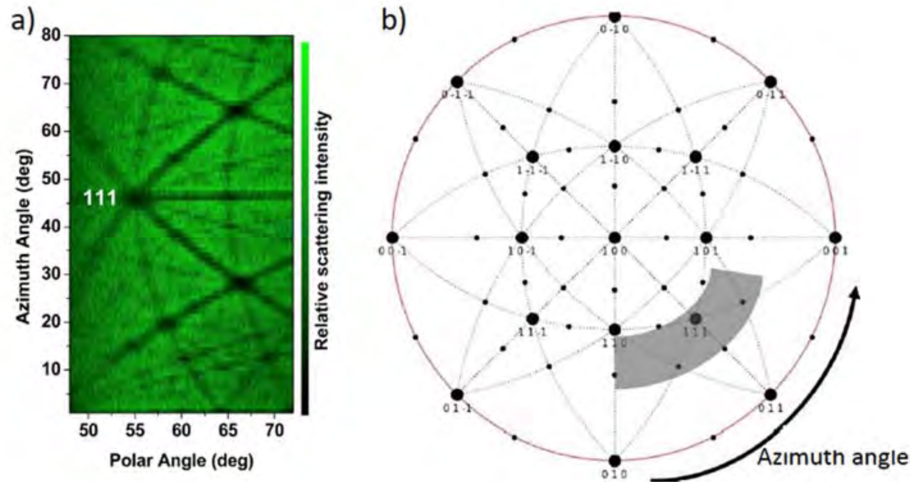

Figure 1 : (a) 2D map of ion scattering intensities as function of the polar and azimuth angle for a Si single-crystal. b) Stereographic projection of a FCC crystal (which encompass the Si crystal) on the [100] direction. The map on the left corresponds to the hachured area on the stereographic plot.

References

[1] D. Jalabert, D. Pelloux-Gervais, A. Bch, J. M. Hartmann, P. Gergaud, J. L. Rouvire, B. Canut, Physica Status Solidi A **209** (2012) 26.

[2] D. Jalabert, J. Coraux, H. Renevier, B. Daudin, M.-H. Cho, K. B. Chung, D. W. Moon, J. M. Llorens, N. Garro, A. Cros, A. Garcia-Cristobal, Phys. Rev. B **72** (2005) 115301.

[3] D. Jalabert, Y. Cur, K. Hestro Y. M. Niquet, B. Daudin, Nanotechnology **23** (2012) 425703.

[4] K. Nakajima, S. Joumori, M. Suzuki, K. Kimura, T. Osipowicz, K. L. Tok, J. Z. Zheng, A. See, B. C. Zhang, Appl. Phys. Lett. 83 (2003) 296.

[5] D. Jalabert, Nuc. Inst. And Meth. in Phys. Res. Section B: Beam Int. with Mat. and Atoms **270**, (2012) 19.

[6] T.S. Avila, P.F.P. Fichtner, A. Hentz and P.L. Grande, Thin Solid Films 2016.

07

Compositional depth profile investigation of plasma doped Si/SiO_2:As by Medium-Energy Ion Scattering

I. Alencar,[1] G.G. Marmitt,[1] P.L. Grande,[1] J.G. England[2], A.K. Rossall[3], and J.A. van den Berg[3]

igor.alencar@ufrgs.br

[1]Instituto de Física, Universidade Federal do Rio Grande do Sul, Porto Alegre, Brazil

[2]Implant Division, Applied Materials, Horsham, UK

[3]International Institute for Accelerator Applications, University of Huddersfield, Huddersfield, UK

In this work, the capability of Medium-Energy Ion Scattering (MEIS) [1,2] to describe nano-structured composites is illustrated. For this purpose, the plasma doping (PLAD) technique for implanting As into Si wafers with a native SiO_2 layer is investigated by MEIS after the samples had been submitted to wet cleaning and thermal treatment processes. Through the analyses of scattering by single and cluster ion beams with the same specific energy and charge state, the Coulomb explosion [3,4] allows the compositional determination as a function of depth by modelling the target structure with the PowerMEIS code [5]. The results are compared to independent measurements made by Transmission Electron Microscopy with Energy Dispersive x-ray Spectroscopy (TEM-EDS).

References

[1] Structural characterization of Pb nanoislands in SiO_2/Si interface synthesized by ion implantation through MEIS analysis. D.F. Sanchez, F.P. Luce, Z.E. Fabrim, M.A. Sortica P.F.P. Fichtner, and P.L. Grande, Surf. Sci. 605 (2011) 654-658.

[2] Structural characterization of CdSe/ZnS quantum dots using medium energy ion scattering. M.A. Sortica, P.L. Grande, C. Radtke, L.G. Almeida, R. Debastiani, J.F. Dias, and A. Hentz, Appl. Phys. Lett. 101 (2012) 023110.

[3] Signatura of plasmon excitations in the stopping ratio of fast hydrogen clusters. S.M. Shubeita, M.A. Sortica, P.L. Grande, J.F. Dias, and N.R. Arista, Phys. Rev. B 77 (2008) 115327.

[4] Neutralization and wake effects on the Coulomb explosion of swift H_2^+ ions traversing thin films. L.F.S. Rosa, P.L. Grande, J.F. Dias, R.C. Fadanelli, and M. Vos, Phys. Rev. A 91 (2015) 042704.

[5] Characterization of nanoparticles through medium-energy ion scattering. M.A. Sortica, P.L. Grande, G. Machado, and L. Miotti, J. Appl. Phys. 106 (2009) 114320.

Passive TiO_2 growth studies using Medium Energy Ion Scattering and Nuclear Reaction Profiling

M. Brocklebank[1], J.J. Noël[2], L.V. Goncharova[1,2]

mbrockle@uwo.ca

[1]Department of Physics and Astronomy, Western University, 1151 Richmond St., London, ON, Canada.
[2]Chemistry Department, Western University, London, ON, Canada

Titanium is used pervasively over a range of fields from medical devices and aerospace, to nuclear plants components [1]. Additionally, its oxide is highly valued for its unique surface properties [2] that can be important for a variety of applications. For example, Ti is ubiquitous in biomedical applications as implants, due to its low reactivity with the surrounding tissues. This is due to the surface properties of a naturally forming oxide on Ti [3]. The oxide is stable thermodynamically and few reactions occur on the surface of the implants. However, many factors can impact this process through modifications of its surface energy: composition, structure, roughness and the tissue or fluid environment [4]. For example, electrochemically formed oxide films on Ti can be amorphous or crystalline, depending on the final anodization potential and electrolyte involved [5]. This can directly affect the biocompatibility of Ti, as thickness and crystallinity (rutile vs. anatase) can affect the degree of adsorption from human blood plasma [6]: i.e. rutile has closer packed structure with less ion diffusion compared to anatase. Thus understanding the oxidation at an atomistic level is necessary if you wish to develop better protective films.

Magnetron sputtering was used to deposit Ti onto Si(001). The Ti film was exposed to isotopic ^{18}O water vapour in Ar atmosphere to form an ultra-thin TiO_2 film in situ. The TiO_2/Ti/Si(001) film was then electrochemically oxidized in $D_2{}^{16}O$ water over a range of voltages from 0-10 V, resulting in ~40–295 Å thick oxide regions. In conjunction with this isotopic labeling, medium energy ion scattering (MEIS) and nuclear reaction profiling (NRP) were used to determine the depth profiles of the ^{16}O and ^{18}O in an attempt to elucidate O transport in the TiO_2. Surface composition was determined using X-ray photoelectron spectroscopy and crystallinity was determined using X-ray diffraction.

Fig.1(b) illustrates how the ^{18}O depth distribution changes as a function of voltage. Initially, ^{18}O accounts for 40% of the O in the ~40 Å oxide.

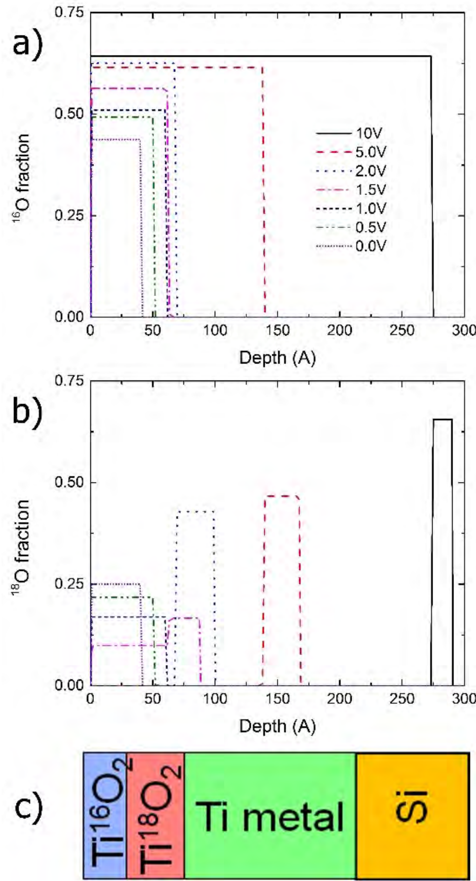

Figure 1: Isotopic depth profiles for (a) ^{16}O and (b) ^{18}O as functions of anodization voltage 0-10 V. These depth profiles are created from simulations of MEIS spectra. Total O concentration for each of these samples is plotted in Figure 2(a). (c) A schematic of the sample involved.

As the anoidization voltage increases, the total concentration of ^{18}O remains constant, which can be seen in Fig.2(b), despite the total oxide thickness increasing monotonically, as seen in Fig.2(a). From to 0.5 V and 1.0 V, the concentration of ^{18}O decreases at the surface and ^{18}O becomes buried deeper. When the voltage reaches 1.5 V, the ^{18}O concentration has decreased at the surface but simultaneously is increasing at greater depths, i.e. new oxide is being created at greater depths. At 2 V, there is no longer any ^{18}O for the first 70 Å of oxide but it accounts for all oxide after that depth, with a stoichiometry $TiO_{0.7}$, which represents a value averaged from oxide and metal phases (i.e. suboxide). From 2 V to 10 V, the depth at which ^{18}O is seen, increases, as does the concentration, but the total amount of the isotope remains constant, confined to an increasingly smaller depth range. At 10 V, all the ^{18}O is confined to a region at 15 Å with a stoichiometry of TiO_2 at a depth of 275 Å into the sample. At this voltage, all the originally sputtered Ti, except for 5 Å (using bulk density), was converted to TiO_2 which is illustrated in Fig.2(b). Thus, oxide forming at deeper depths is due to the transport and incorporation of ^{18}O.

Consistent with the transport of ^{18}O are the depth profiles of ^{16}O, which are presented in Fig.1(b). From Fig.2(a) the ^{18}O concentration can been seen to remain constant, while the ^{16}O concentration rises monotonically as a function of voltage, consistent with the increase in

prevalence of Ti in an oxide phase. Thus increasing incorporation of ^{16}O is the reason for the oxide growth at the oxide-environment interface and given the simultaneously decreasing concentration of ^{18}O, the mechanism for new oxide growth at the oxide-environment interface is through exchange.

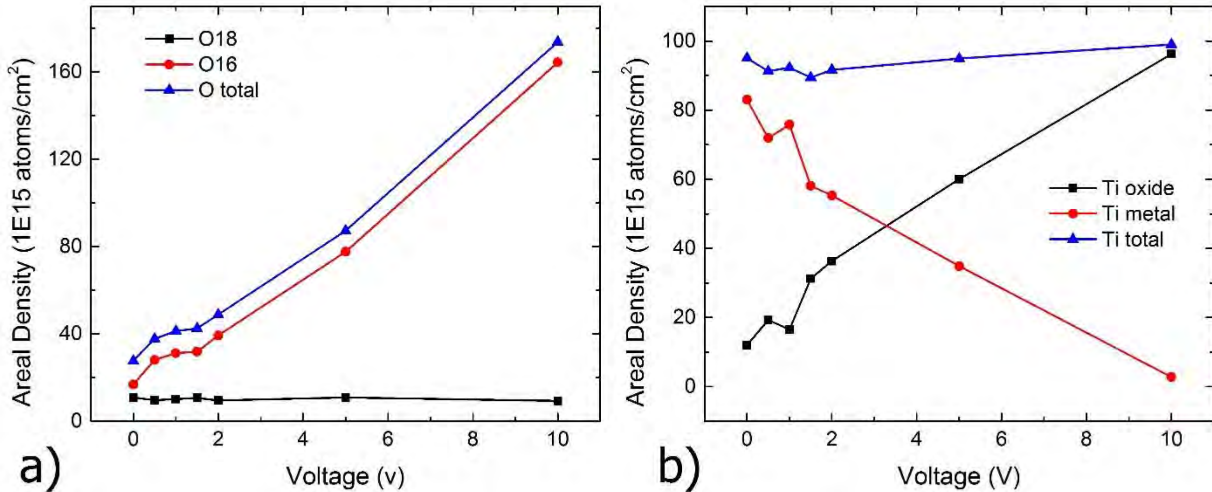

Figure 2: The change in for composition as a function of oxidizing voltage in the anodized Ti: (a) Oxygen exchange curves (b) Total Ti concentration and prevalence of Ti in both the oxide and the metal phases.

Thus, oxide growth increases as function of voltage with increasing incorporation of ^{16}O towards the oxide-environment interface, while ^{18}O is transported to greater depths (while the total amount of ^{18}O remains constant) implying that this occurs via O exchange reactions. Simultaneously new oxide is created by ^{18}O being transported towards the oxide/metal interface, all of which is consistent with O ions as a mobile species but additionally with the possibility Ti ions may be transported towards the oxide-oxidant interface.

References:

[1] The uses of titanium. J.R.B. Gilbert. Mat. Sci. and Tech. 1 (1985) pp 257-262

[2] The surface science of titanium dioxie. U. Diebold. Surface science reports 48 (2003) pp 53-229

[3] Spectroscopic characterization of passivated titanium in a physiologic solution. J.L. Ong, L.C. Lucas, G.N. Raikar, R. Connaster, J.C. Gregory. J. Mater Sci. Mater Med. 6 (1995) pp 113-116

[4] A comparison of the surface characteristics and ion release of Ti6Al4V and heat-treated Ti6Al4V. T.M. Yang, E. Chang, and C.Y. Yang. J. Biomed. Mater Res. 50 (200) pp 499-511

[5] Potentiodynamic behavior of mechanically polished titanium electrodes. O.R. Camara, C.P. Pauli, M.C. Giordano. Electrochimica Acta 29 (1984) pp 1111-1117

[6] Formation and characteristics of the apatite layer on plasma-sprayed hydroxyapatite coatings in simulated body Fluid. J. Weng, Q. Liu, J.G. Wolke, X. Zhang, K. de Groot. Biomaterials 18 (2997) pp 1027-1035

09

Application of ERBS analysis on O diffusion in TiO_2 films

G.G. Marmitt[1], S.K. Nandi[2], D.K. Venkatachalam[2], R.G. Elliman[2], M. Vos[3] and P.L. Grande[1]

gabriel.marmitt@ufrgs.br

[1] Instituto de Física, Universidade Federal do Rio Grande do Sul
[2] Electronic Materials Engineering Department, The Australian National University
[3] Atomic and Molecular Physics Laboratories, The Australian National University

Electron Rutherford Backscattering (ERBS) is a technique that depends on the recoil energy transferred from the scattering electron to a nucleus in a large-angle deflection. This energy transfer depends on the mass of the scattering atom. Analysing the energy of the scattered electrons reveals thus which atoms are present in the near surface layer [1, 2].

In simple cases where there are 2-3 separate peaks due to different elements that do not overlap one can simply fit the spectra with the corresponding number of Gaussians. In more complicated cases the peaks overlap and a unique fitting of the spectrum based on a larger number of Gaussians can not be obtained. Besides the composition of each layer it is then of interest to measure their thickness. The added complexity usually require the measurement of the sample under different geometries and/or incoming energies and the simultaneous analysis of all spectra. As this work shows, fitting of the data allows for very precise thickness and compositional determination. Among other examples [3], the analysis of a Si_3N_4 layer on TiO_2 is particularly interesting. In this case the peaks overlap strongly, and show that highly consistent estimates of the thickness of the Si_3N_4 film are obtained for different measurement geometries.

This procedure was then applied to the study of oxygen auto-diffusion through the use of isotopic marking, in an attempt to obtain the depth profile distribution attributed to the diffusions. High-resolution measurement of the energy of electrons backscattered from oxygen atoms makes it possible to distinguish between ^{18}O and ^{16}O isotopes as the energy of elastically scattered electrons depends on the mass of the scattering atom.

Oxygen diffusion in TiO_2 is of particular interest, because it is the material that has received most work in memristors and is a well studied system within ReRAMs (resistive random access memories) [4]. Conventional ion-beam techniques are capable of such resolution but require particular care to ensure that radiation damage does not contribute to the measurement. Here we address these limitations by employing an electron-scattering technique to measure interdiffusion in $Ti^{16}O_2$ / $Ti^{18}O_2$ and $Ti^{18}O_2$ / $Ti^{16}O_2$ bilayers.

Thermal annealings for 5 minutes at 500 – 800°C in Ar atmosphere were conducted on our samples. Under these conditions, we were able to determine the activation energy for O self-diffusion in TiO_2 at about 0.9 eV. By thermally treating samples for different times (5 – 100 min.) at a fixed temperature (650°C), the diffusion regularity was also studied. The Arrhenius plot of diffusion length versus time exhibits two regions, suggesting that different diffusion mechanisms are involved.

References.

[1] M. Went and M. Vos, Appl. Phys. Lett. 90, 072104 (2007).
[2] M. Went and M. Vos, Nuclear Instruments and Methods in Physics Research Section B 266, 998 (2008).
[3] G.G. Marmitt, L.F.S. Rosa, S.K. Nandi, and M. Vos, J. Electron Spectrosc. Relat. Phenom. 202, p. 26–32 (2015).
[4] E. Gale, Semicond. Sci. Technol. 29, 104004 (2014).

International RRT of MEIS analysis of HfO_2 thin films and multiple delta layers

D.W. Moon[1], P.L. Grande[2] G.G. Marmitt[2] and RRT participants

dwmoon@dgist.ac.kr & grande@if.ufrgs.br

[1] *Department of New Biology, DGIST, TechnoDaeRo 333, Dalsung, Daegu, Korea 711-873*
[2] *Instituto de Física, Universidade Federal do Rio Grande do Sul, Avenida Bento Gonçalves 9500, 91501-970 Porto Alegre, Rio Grande do Sul, Brazil*

Scattering cross sections, electronic stopping power, and straggling are important parameters in MEIS analysis. Most of the equations to calculate these parameters in MEIS analysis can be considered to be extended from high energy scattering, even though these parameters in MEIS analysis were tested for certain cases. Recently, with development of MEIS system instrumentation, wider ranges of ion beam energy, ion species, and ion analyzer were used. We tried to see the consistency of MEIS analysis results and to find out the most accurate MEIS parameters for various MEIS analysis conditions.

2015, the 1st RRT were performed with 1, 3, 5, 7 nm HfO_2 thin films. To our surprise, quite large scattered values of HfO_2 thickness or the amount of Hf as large as 20~30% were observed. Couple of possible causes were suggested and discussed. We decided to run 2nd RRT with a slightly modified sample structure and additional multiple HfO2 delta layers for a more accurate estimation of MEIS parameters, which is in progress.

In this presentation, we will report all the RRT results of MEIS spectra from participants and the corresponding data analysis using the PowerMeis software. The 1st RRT and 2nd RRT will be used to find out any source of errors in MEIS analysis and the most accurate MEIS analysis parameters over the MEIS analysis conditions via active discussions from participants and HRDP attendants.

The results will be reported to ISO/TC201/SC4 Depth Profiling probably to develop a standard in MEIS analysis.

11

He Ion Microscopes: Potential and pitfalls

L.C. Feldman[1,3] T. Gustafsson[1,3], V. Manichev[1,2] , H. Wang[1,3]

l.c.feldman@Rutgers.edu

[1]Institute for Advanced Materials, Devices and Nanotechnology
[2]Department of Chemistry and Chemical Biology;
[3]Department of Physics and Astronomy, and Laboratory for Surface Modification, Rutgers University, Piscataway, NJ, USA

The He Ion Microscope (HIM) produces a sub-nanometer spot size with a beam energy between 20-35 KeV. The tool brings the ion beam community to the real nanoscale regime in a commercially available tool.

The main uses of the apparatus are: 1) imaging via secondary electron emission, 2) ion beam lithography and 3) ion beam machining on the nanoscale. In addition various groups are developing element identification tools operable at the nanoscale, nanoscale writing via radiation enhanced CVD, and unique transmission geometries to look for thin crystal channeling. A variety of successful examples of HIM use will be given in the following talks. Some examples from the Rutgers laboratory include:

1) Collaborative projects in the biological and biomedical fields.
2) Development a Time-of-Flight system capable of element identification.
3) He beam induced single atom defects in MoS_2 and their effects on the host lattice.
4) Machining of SiC for structured graphene growth and stress regulation in graphene.
5) Selective defect production in 2D material such as MoS_2.

Successful operation depends on a thorough knowledge of the particle-solid interaction familiar to those in the field. The advantages of the HIM for imaging are directly connected to the decrease of multiple scattering at the surface as compared to electron beams. HIM imaging makes use of the secondary electron emission, but is limited by ion beam induced damage. Ion beam machining makes use of macroscopic and microscopic defect production associated with the ion beam-solid interaction but now at the nanometer level.

While a number of successes currently exist (see the following talks) more precise knowledge of ion beam solid physics is required to bring the tool to the desired level of quantitative use. These include issues such as a quantitative basis of electron emission, the so called non-charging effects, electron emission associated with large angle scattering events, the formation of sub-surface “blisters” and the blister dependence on material type, ion beam sputtering and electron emission dependence on doping in semiconductors. In addition to these factors the challenges associated with element analysis will be discussed.

This work was supported by Rutgers Institute for Advanced Materials, Devices and Nanotechnology, NSF grant DMR-1126468, and DOE grant DE-FG02-93ER14331.

Ion beam analysis in a Helium Ion Microscope – elemental mapping on the nm scale

N. Klingner[1], **R. Heller**[1], G. Hlawacek[1], P. Gnauck[2], S. Facsko[1] and J.v. Borany[1]

r.heller@hzdr.de

[1]Helmholtz-Zentrum Dresden-Rossendorf, Institute of Ion Beam Physics and Materials Research, Bautzner Landstr. 400, 01328 Dresden, Germany
[2]Carl-Zeiss-Microscopy GmbH, D-73447 Oberkochen, Germany

In recent years Helium Ion Microscopes (HIM) rapidly have become commonly used high resolution imaging devices in laboratories all over the world. Beside a sub nanometer resolution and a high depth of field the latest generation of HIM devices (Zeiss Orion NanoFab) can be operated with both helium and neon ions as well and thus offer various opportunities for local surface modifications [1].

While the image generation in a HIM is realized by evaluating the amount of secondary electrons (SE), the energy of backscattered He or Ne projectiles was rarely taken into consideration so far. However, this energy contains information on the elemental composition of the surface and the sub-surface region and it thus provides an additional mechanism for contrast generation. Early attempts to measure BS energy spectra were carried out by Sijbrandij et al. [2] and gave evidence for the general feasibility but also revealed that a quantitative element analysis of thin layers would require the development of more sophisticated detection concepts.

In this contribution we present an experimental approach and the corresponding results of backscattering spectrometry (BS) in a HIM with a lateral resolution < 55 nm and an energy resolution < 3 keV (example seen in fig. 1). We show that pulsing the primary ion beam and measuring the Time-of-Flight (ToF) of the backscattered He/Ne enables BS spectrometry in a HIM without disturbing its excellent imaging capabilities [3]. Since our approach enables us also to perform Secondary Ion Mass Spectrometry (SIMS) by biasing the sample to a positive or negative potential, elemental contrast in chemical analysis is further increased.

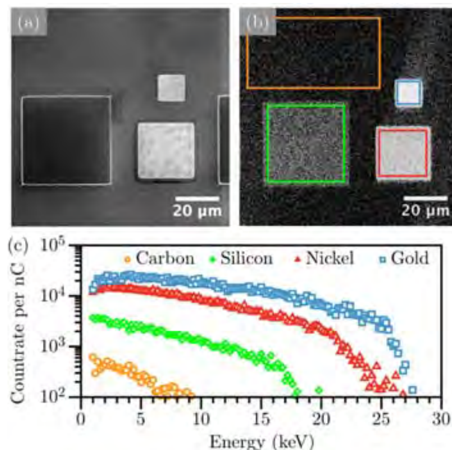

Figure 1: Images of a carbon sample covered with rectangular patterns of Si, Ni and Au acquired in standard SE mode (a) and in ToF-BS mode (b). The color scale in (b) corresponds to the time of flight of the BS particles. In contrast to SE imaging this technique reveals well-defined elemental contrast. ToF-BS spectra obtained from different regions in (b) - marked by rectangles - are plotted in (c). The color of the spectra equals the color of the rectangles in (b). The ToF-BS spectra allow clearly to distinguish between different elements.

Both techniques - SIMS and BS - in conjunction with the high-resolution imaging by SEs reveal a "complete" picture of the sample in terms of topography and chemistry. Additionally, the evaluation of BS spectra opens access to investigate the sub-surface chemistry by measuring elemental depth profiles.

[1] G. Hlawacek, V. Veligura, R. van Gastel and B. Poelsema, J. Vac. Sci. Technol. B **32** (2014) 020801

[2] S. Sijbrandij, B. Thompson, J. Notte, B. W. Ward and N. P. Economou, J. Vac. Sci. Technol. B **26** (2008) pp 2103-2106

[3] N. Klingner, R. Heller, G. Hlawacek, J. von Borany, J. Notte, J. Huang and S. Facsko, Ultramicroscopy **162** (2016) pp 91-97

Helium Ion Microscopy studies of biological/biomedical samples, atomic size defects and elemental identification

V. Manichev[1], E. Garfunkel[1], J. Yang[2,3], M. Chhowalla[2,3], M. Lagos[2,3], P. Batson[2,3,4], L.C. Feldman[3,4] and T. Gustafsson[4]

slavamani@gmail.com

[1] Department of Chemistry and Chemical Biology
[2]Department of Materials Science and Engineering
[3]Institute for Advanced Materials Devices and Nanotechnology,
[4]Department of Physics and Astronomy, and Laboratory for Surface Modification
Rutgers University, Piscataway, NJ 08854, USA

a. Using Helium Ion Microscope, we are pursuing collaborative projects in the biological and biomedical fields. We have imaged “aged” rat kidney glomeruli, the biological structure responsible for blood filtration. Our images clearly show structural and morphological changes associated with the aging process. We have also investigated the effect of ocean acidification on coral survivability. We have imaged calcification centers in corals and observed significant morphological changes as calcium is absorbed.

b. Our lab has a substantial experience working with ion beam techniques like RBS and MEIS where elemental identification is done routinely with great accuracy. We are developing a Time-of-Flight system capable of energy discrimination in the Helium Ion Microscope. This detector will bring elemental identification to the subnanometer regime. A proof-of-principle experiment will be presented.

c. The new Rutgers UltraSTEM microscope allows the formation of an angstrom-size monochromatic electron beam. With this capability, spatially-resolved spectroscopy studies over a wide energy range (from vibrational excitations to core-shell transitions) can be conducted in nano-sized systems. We will present results on He beam induced single atom defects in MoS_2 and their effects on the host lattice.

This work was supported by Rutgers Institute for Advanced Materials, Devices and Nanotechnology, NSF grant DMR-1126468, and DOE grant DE-FG02-93ER14331.

14

Electronic interactions of medium-energy ions with solids: some recent results and their implications for high-resolution depth profiling

D. Primetzhofer

daniel.primetzhofer@physics.uu.se

Physics and Astronomy, Uppsala University, Box 516, SE-75120 Uppsala, Sweden

Both qualitative and quantitative understanding of the electronic interactions of ions at energies of a few up to several hundred keV is of decisive importance for quantitative material analysis employing ions in the present energy regimes. For example, only accurate knowledge on charge exchange processes permits to employ a method like Low-energy Ion Scattering as a tool to probe the composition of the outermost atomic layer of solids. On a similar basis, inaccuracies in the description of the energy loss experienced along ion trajectories in the solid lead to difficulties in establishing quantitative depth profiles in e.g. Medium-Energy Ion Scattering (MEIS) or other near-surface depth profiling techniques.

Although investigated for a long period of time an accurate prediction of the absolute magnitude of the energy loss per unit path length, the stopping power $S = dE/dx$, is often not straightforward possible. This complication has several reasons: at first, the increased contribution from nuclear losses requires more advanced evaluation routines for deducing reference data, as compared to the MeV-energy regime. Second, the description of the electronic energy loss is complicated by the increased weight of the valence electrons which are sensitive to the chemical surrounding and by the fact, that the interaction is no longer adiabatic, requiring consideration of e.g. dynamic screening phenomena or complex charge exchange processes. Finally, for thinner targets higher relative weight of the near-surface regions of the target materials makes high standards during preparation and accurate knowledge on sample composition an ultimate requirement for obtaining high quality data.

In this contribution recent studies of the energy loss of light and heavy ion in the energy regime from about 10 to about 300 keV performed at Uppsala University are presented to exemplify some of the above mentioned complications in analysis, the complexity of the obtained results as well as the necessity of extensive sample characterization, also for relatively simple systems.

As a first example, a study of the energy loss of Ne ions in Au, Pt and Ag is presented [1]. The presented investigations were performed to obtain a better understanding of the relative contributions of electronic and nuclear energy losses to the experimental spectra. Thin films of the materials of interest were prepared by sputter deposition on Si-substrates. Thickness calibration and characterization of the thin films was performed ex-situ by means of Rutherford Backscattering Spectrometry (RBS) and Time-of-Flight Elastic Recoil Detection Analysis (ToF-ERDA). Ne ions with energies between 80 and 280 keV were scattered from the targets and detected in backscattering direction by a position-sensitive detector with a large solid angle in a Time-of-Flight Medium Energy Ion Scattering (ToF-MEIS) set-up [2]. The present approach allows for high energy resolution and only minor sample deterioration due to the low employed primary particle dose. Spectra of backscattered particles were analyzed with help of the Monte-Carlo program TRim for BackScattering (TRBS) [3]. A typical spectrum as obtained in the present study is shown in Fig. 1. Both the high-energy onset and a pronounced tail towards lower energies show the prominent contribution due to multiple scattering to the experimental yield, also at the highest particle energies. The figure illustrates the accuracy of the simulations

in reproducing the experimental results for correct choice of the scattering potential (red line for the Thomas-Fermi-Molière potential - TFM). Note, however, that in the simulations multiple scattering is strongly influenced by the exact choice of the potential (see dashed lines in the figure for the use of different screening length corrections c_a). Changes in the electronic stopping employed in the simulations are found to influence mainly the width of the spectrum (not shown) and permit thus to extract electronic stopping cross sections ε from a best fit to the experiment with accurate settings for the scattering potential.

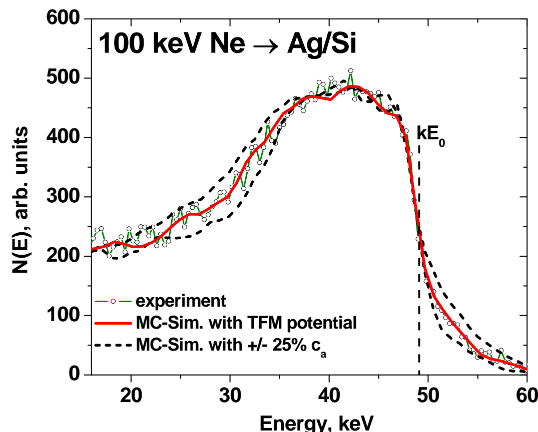

Figure 1: Energy-converted spectrum recorded for 100 keV Ne primary particles scattered from a thin film of Ag/Si (open symbols). The spectrum shape is strongly influenced by multiple scattering. The red continuous and the black dashed lines show simulated yields obtained by TRBS for the Thomas-Fermi-Molière potential without and with ±25% screening length correction.

In parallel to the quantification of ε with help of the MC-simulations, a simple evaluation within the single scattering model was performed to compare for the influence of multiple scattering and the nuclear energy loss. This comparison of different evaluation strategies was motivated by observed discrepancies between the recent results obtained in backscattering and earlier results by different groups in transmission experiments. The results of the present study show that for both, transmission and backscattering spectra, the ratio of electronic to nuclear stopping observed along the relevant trajectories significantly deviates from the tabulated values. The performed evaluation together with TRIM calculations shows that also in backscattering experiments the nuclear stopping contributions are found significantly smaller than expected along random trajectories. These results indicate an efficient trajectory selection process when evaluating spectra in typical experiments performed to extract information on the inelastic energy loss. Note, that the present results for Ne and about 100 keV primary energy also indicate that equivalent considerations can be expected to be valid for scattering of Helium at energies around or below 10 keV as well as for protons for energies around and below a few keV where similar strong multiple scattering contributions to the spectrum can be expected.

A second set of experiments was designed to study the energy loss of hydrogen and helium in in a material of high relevance for the MEIS community, i.e. HfO_2. HfO_2 was grown by atomic layer deposition on Si with a 0.5 nm thick SiO_2 buffer layer. A thorough characterization of the material system was performed in order to avoid artefacts from e.g. inaccurate stoichiometry of the oxide [4]. A combined approach via elastic resonance scattering around the resonance at 3.0375 MeV for oxygen together with channeling experiments at MeV energies was used to confirm the correct stoichiometry.
The experiments performed to measure the electronic stopping cross section ε [5] revealed a difference in the magnitude and the velocity dependence of the energy loss observed for H and He ions that goes beyond explanations based on the electron density of valence electrons in the system.
Figure 2 shows the observed electronic stopping cross sections normalized with the projectile velocity, yielding a friction coefficient Q according to $\varepsilon = Q \cdot v$. Experimental data for protons

and helium is shown as full squares and asterisks respectively. Also shown are predictions for Q in a free electron gas (FEG) as obtained from DFT for equivalent electron density for H and He (dashed and dash-dotted lines respectively), expressed by the density parameter r_s [6]. The electron density for the shown curves is equivalent to 3.7 electrons per molecule (obtained from fitting to the data for H). Obviously, DFT-predictions based on the electron density obtained for H is not matching data for He. Instead, for helium, a density of the FEG equivalent to 11 e^- per molecule is necessary to explain the observed difference in magnitude of the electronic stopping cross section at a given ion velocity. Additionally, data for He shows less clear velocity proportionality at velocities below 1 a.u, for which DFT calculations are expected to be most applicable. Thus, even if the employed DFT-predictions for a FEG are definitely not fully applicable for a large-band insulator such as HfO_2, the present results are a strong indication for processes different from electron-hole pair excitation contributing to the energy loss of He ions in HfO_2.

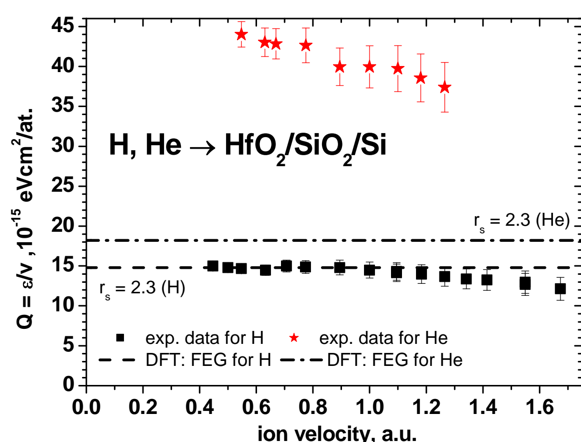

Figure 2: Electronic stopping cross sections for H and He ions in HfO_2 normalized with the projectile velocity (full squares and asterisks, respectively). Also shown are DFT predictions (dashed and dash-dotted lines).

A detailed comparison of the results with those for other materials such as SiO_2 yields further evidence for a contribution to the inelastic energy loss which is influenced by both the presence of the oxygen 2s-bands as well as the Hf 4f-states: for SiO_2 and HfO_2, the specific energy loss of protons is found almost identical for energies where f-electrons likely do not participate in direct excitations, which is a strong indication, that energy dissipation is mainly due to excitation of O-2p-like states, which are the dominant contribution to the density of states at low binding energies in both system. Also for SiO_2, however, He shows increased specific energy loss with respect to DFT-predictions. The effect, however, is found less pronounced which may be based in the fact, that also f-states affect the energy loss for He in HfO_2.

References:

[1] M.K. Linnarsson, A. Hallén, J. Åström, D. Primetzhofer, S. Legendre, G. Possnert, Rev. Sci. Instrum. 83 (2012) 095107.
[2] J.P. Biersack, E. Steinbauer, P. Bauer, Nucl. Instr. Meth. B61 (1991) 77.
[3] S.R. Naqvi, G. Possnert, D. Primetzhofer, Nucl. Instr. Meth. B 371 (2016) 76
[4] C. Zoller, E. Dentoni-Litta, D. Primetzhofer, Nucl. Instr. Meth. B 347 (2015) 52
[5] D. Primetzhofer, Phys. Rev. A 89 (2014) 032711
[6] I. Nagy, A. Arnau, and P. M. Echenique, Phys. Rev. A 40 (1990) 987

15

MEIS studies of oxygen plasma cleaning of copper for fast response time photocathodes used in accelerator applications

T.C.Q. Noakes[1], S. Mistry[2], M.D. Cropper[2], **A.K. Rossall**[3], J.A. van den Berg[3]

tim.noakes@stfc.ac.uk

[1] STFC Daresbury Laboratory, SciTech Daresbury, Keckwick Lane, Daresbury, Warrington, WA4 4AD, UK
[2] Department of Physics, Loughborough University, Loughborough, LE11 3TU, UK
[3] International Institute for Accelerator Applications, University of Huddersfield, Queensgate, Huddersfield, HD1 3DH, UK

The performance of a fourth generation light source is to a greater extent reliant on the properties of the electron bunches, with the fundamental limit controlled by the photocathode where the electrons are emitted. Normally conducting RF guns often use metal photocathodes, mainly due to their fast response time that allows very short pulses to be generated. However, they typically have very low quantum efficiency (QE) compared to semiconductor alternatives (GaAs or Cs_2Te). The drive to use higher QE metals is motivated by the need to minimize the laser power required to generate sufficient bunch charge for the downstream accelerator.

The use of Cu as the metal photocathode of choice is long standing. However, the preparation of an atomically clean surface is thought to be key to achieving a high enough QE to be used in an RF gun. At STFC Daresbury laboratory a preparation procedure has been developed that has allowed a QE of approximately 10^{-5} to be achieved. This coupled with a high power UV laser system has allowed electron bunches of up to 250 pC to be generated in the Versatile Electron Linear Accelerator (VELA) facility [1]. However, there is very little understanding of how the cleaning procedure leads to the required surface properties for electron emission and hence a detailed study has been initiated.

The experiments were carried out using 99.99% purity polycrystalline copper samples with an ‘as rolled’ surface finish. Oxygen plasma treatment of the copper samples was carried out using a Henniker Plasma HPT-200 system, which is fed using 99.998% pure oxygen. However, the actual purity of the gas during operation is likely to be limited by the ultimate pressure of the scroll pump used for evacuating the chamber, which is around 0.1 mbar. The two parameters which can be varied for the plasma treatment are the power level and the treatment time. Power levels of between 10 and 100% were evaluated, along with treatment times of between 5 and 20 minutes. Samples were removed from the plasma chamber and transferred in air to the UHV MEIS analysis system. Post treatment annealing of the samples was carried out in the separate preparation chamber using radiative heating at lower temperature of 300°C and electron bombardment heating for the higher temperature of 600°C.

MEIS analyses were carried out using the newly re-established UK instrument in the International Institute for Accelerator Applications at the University of Huddersfield (see Fig.1). Whilst the ion source and beam line has been completely reconfigured, the end station equipment, including the analysis chamber remains essentially unchanged from its previous incarnation at Daresbury [2]. The analyses were performed using 100 keV He ions with a spot size of 0.5 x 1.0 mm and a dose of 1.25 µC per tile. The beam was moved to a different spot on the sample at regular periods during analysis to avoid damage buildup. Since the samples were amorphous, a piece of

crystalline silicon was first inserted into the beam and used to ensure that the detector was at 90° scattering angle. The incidence angle of the beam on target was set at 35.3° for all the samples analyzed.

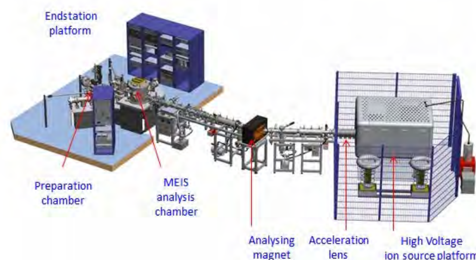

Figure 1: MEIS Instrument at the University of Huddersfield

Data analysis was carried out using the SIMNRA 5.02 code [3]. This version is preferred over more recent versions because of its capability for fitting layer thickness and composition independently. The data were fitted using a four layer model where the bottom layer is essentially bulk pure copper which allows the calibration of particles per steradian to be fitted. The top layer was fixed at approximately five monolayers thickness and the composition allowed to vary to produce a fitted value for the composition at the very surface. The subsequent layer, which represents the majority of the oxide layer, was allowed to have both variable thickness and composition. Finally, there is an interfacial layer between the film and the bulk. This layer probably has gradually varying composition, but is modelled by a single composition with some film roughness added to smear out the signal and improve the fit. From the perspective of understanding the effect of oxygen plasma treatment, the important parameters are the total film thickness and the composition of the film and surface region.

Data for the surface region were typically very similar to the oxide film beneath, with if anything a slight depletion in oxygen for some samples. The thickness of the oxide layer showed the expected dependence on treatment time with a significant increase as the time increased. The observed dependence of film thickness on plasma power was less expected, since there was a maximum at around 50% power level, after which there was a gradual decline. Annealing the films to around 300°C gave rise to an overall reduction in the oxygen content, without much change in the film thickness. Annealing to 600°C appeared to remove all the oxygen from the surface region leaving pure copper.

In practice, the photocathodes used in VELA are only annealed to 250°C after oxygen plasma treatment and loading into the gun vacuum system, although they are held at this temperature for over a week. It is therefore unlikely that a completely oxygen free surface is produced. It can be speculated that the high-power UV laser used during operations also has some cleaning effect and further analyses are required to investigate this potential effect.

References.

[1] B.L. Militsyn et al, *'Beam physics commissioning of VELA at Daresbury Laboratory'* Proceedings of the International Particle Accelerator Conference 2014 (IPAC-14), THPRO052, 2014, Dresden , Germany

[2] P. Bailey, T.C.Q. Noakes and D.P. Woodruff *'A medium energy ion scattering study of Sb overlayers on Cu(111)'* Surface Science 426 (1999) 358

[3] M.Mayer, *'SIMNRA User's Guide'* Report IPP9/113, Max-Planck-Institut fur Plasma Physik, Garching, Germany, 1997

Nuclear Reaction Profiling unraveling the incorporation of water in SiO_2/SiC structures

F.C. Stedile[1,2], E. Pitthan[2], S.A. Corrêa[1], G.V. Soares[2,3], and C. Radtke[1,2]

fernanda.stedile@ufrgs.br

[1]*Instituto de Química - Universidade Federal do Rio Grande do Sul, Av. Bento Gonçalves, 9500, 91501-970, Porto Alegre, RS, Brazil*

[2]*PGMICRO - Universidade Federal do Rio Grande do Sul, Av. Bento Gonçalves, 9500, 91501-970, Porto Alegre, RS, Brazil*

[3]*Instituto de Física - Universidade Federal do Rio Grande do Sul, Av. Bento Gonçalves, 9500, 91501-970, Porto Alegre, RS, Brazil*

Silicon carbide (SiC) is a wide-band-gap semiconductor suitable for applications under extreme conditions. SiC-based metal-oxide-semiconductor field-effect transistors (MOSFETs) are expected to be a key component for next generation green electronics. However, to exploit its potential, reliable devices must be achieved. The presence of water-related species might be a source for instabilities during devices operation, as it was already reported for silicon-based devices. However, this is still a neglected factor for the technology based on SiC.

In this work, we report the use of ion beam analyses as an effective method to unravel the incorporation process of water vapor in silicon dioxide (SiO_2) films on SiC or Si substrates. To increase sensitivity and selectivity for quantification and profiling of hydrogen and oxygen, water isotopically enriched (termed heavy water) simultaneously in deuterium (^{2}H or D) and in ^{18}O was used, assuming that they mimic ^{1}H and ^{16}O, respectively, which are the most abundant of these nuclides in nature. The use of the rare isotopes ^{18}O and D (natural abundances of 0.205 and 0.015%, respectively) allows one to distinguish them from O and H incorporated during air exposure and/or from nuclides present in the isotopically natural SiO_2 film. SiO_2 films were deposited by RF sputtering on SiC or on Si wafers and/or thermally grown at 1100ºC in 100 mbar of dry natural O_2. Samples were afterwards submitted to annealings in 10 mbar of heavy water vapor for 1 h at temperatures ranging from 20 to 1000ºC. The water vapor pressure used in these annealings corresponds approximately to the water partial pressure in air with 30% relative humidity at 25ºC, typical of a clean room.

The incorporation of water in SiO_2 films was investigated using Narrow Nuclear Reaction Profiling (NNRP), Nuclear Reaction Analysis (NRA), and Rutherford Backscattering Spectrometry (RBS). ^{18}O profile and quantification were determined by using the narrow resonance (Γ~100 eV) and the plateau in the cross section curve of the ^{18}O(p,α)^{15}N nuclear reaction at 151 keV and at 730 keV, respectively. D quantification was accomplished by NRA, using and the D(^{3}He,p)^{4}He nuclear reaction at 700 keV. The areal density of ^{16}O was determined by RBS in channeling geometry (c-RBS). The profiling of D was obtained by combining step-by-step dissolution of the oxide film in a diluted HF aqueous solution with D and (^{18}O+^{16}O) quantifications by NRA and c-RBS.
In a first moment, SiO_2 films with thicknesses in the 6 to 50 nm range were thermally grown in

dry natural O_2 on SiC or on Si wafers. ^{18}O profiling reveals that in all $D_2{}^{18}O$ annealing temperatures, ^{18}O is incorporated in the oxide films until reaching the SiO_2/SiC interface. In contrast, the incorporation in SiO_2/Si structures occurs only in the near surface region for water exposure temperatures between 20 and 600ºC. Annealing at 1000ºC allowed ^{18}O to reach the SiO_2/Si interface forming $Si^{18}O_2$ due to the reaction between oxidant species and the Si substrate [1]. Concerning D incorporation, results shown in Fig.1 evidence its presence in the surface, bulk, and interface regions of SiO_2/SiC structures, whereas in the case of SiO_2/Si, it is observed only in near-surface regions of the oxide film [2]. Besides, higher incorporation of D was observed in SiO_2/SiC structures as compared to those of SiO_2/Si at temperatures above 600ºC, which can lead to electrical instabilities in the formers, especially in devices that operate at high-temperatures.

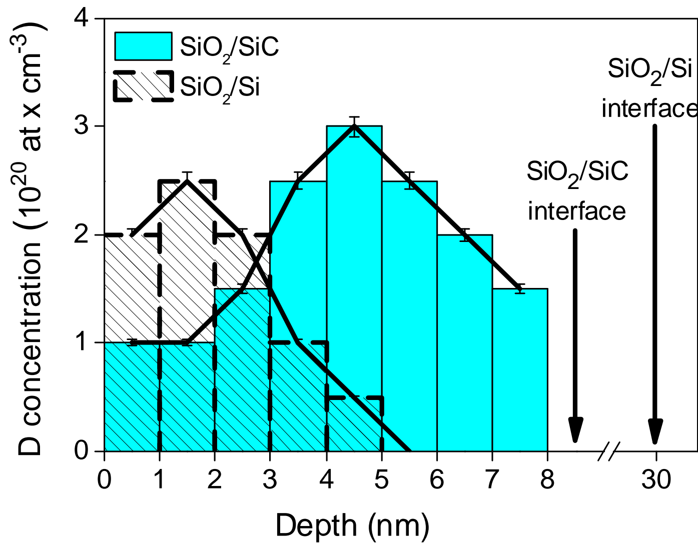

Figure 1: Deuterium profiles in natural SiO_2 films, initially 6 nm thick, thermally grown on SiC (cyan columns) and Si (dashed columns) after thermal treatment in $D_2{}^{18}O$ at 1000ºC. The positions of new film/substrate interfaces are indicated in both cases. Lines are only to guide the eyes.

The route employed to obtain SiO_2 films on SiC was observed to affect the electrical characteristics of the SiO_2/SiC interface, which is key for MOS devices [3]. Thus SiO_2 films were either deposited by RF sputtering or thermally grown on SiC wafers. The longer the thermal oxidation, the more degraded were the electrical properties of the SiO_2/SiC interfacial region. Additional samples were synthesized using short oxidation times and then covered by a deposited SiO_2 film. In a following step, all samples were submitted to annealing in heavy water. Isotopic exchange between oxygen from the water vapor and oxygen from SiO_2 films deposited on SiC was observed in the whole depth of the films, differently from the behavior of SiO_2 films thermally grown on SiC, where it occurs mainly in the surface region of the film [4].

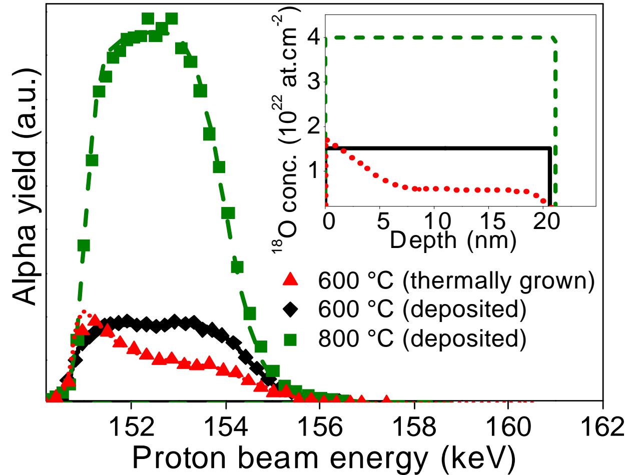

Figure 2: Experimental (symbols) excitation curves of the $^{18}O(p,\alpha)^{15}N$ nuclear reaction around the resonance at 151 keV and the corresponding simulations (lines) for a SiO_2 film 20 nm thick thermally grown on SiC submitted to $D_2{}^{18}O$ annealing at 600ºC and for SiO_2 films ~23 nm thick deposited by sputtering and submitted to $D_2{}^{18}O$ annealings at 600 or at 800ºC . **Inset:** ^{18}O profiles obtained in the simulations using the same line types. 4×10^{22} $^{18}O/cm^3$ corresponds to the oxygen concentration in stoichiometric SiO_2.

The incorporation of hydrogen from water vapor in SiO_2/SiC and SiO_2/Si structures, whose films were deposited by sputtering, occurred mainly in the SiO_2 film/substrate interfacial region. Longer thermal oxidations of the SiC prior to the deposition of the SiO_2 film led to larger amounts of D incorporated. The thermal growth of a very thin SiO_2 film followed by the deposition of SiO_2 led to the lowest amounts of D incorporated. These results were accompanied by the improvement in the electrical characteristics observed for SiO_2/SiC structures obtained by these routes, suggesting that the D incorporation occurs in defects in the structure that exist prior to the water vapor annealing. As a consequence of the annealing, a significant reduction in the negative effective charge in MOS capacitors and the removal of the SiO_2/SiC interfacial region was observed, which were assigned to the reduction of the amount of silicon oxycarbide (SiO_xC_y) compounds in the interfacial region.

As a general conclusion, our results indicate that strict control of water vapor contents in SiO_2/SiC is mandatory in order to achieve further improvements in the SiC-based device technology.

References

[1] G.V. Soares *et al.* Appl. Phys. Lett. **95** (2009) 191912-1

[2] S.A. Corrêa *et al.* Nucl. Instrum. Meth. B **273** (2012) 139

[3] E. Pitthan *et al.* ECS Solid State Letters, **2** (2013) P8

[4] E. Pitthan *et al.* Appl. Phys. Lett. **104** (2014) 111904

17

Detection of hydrogen in steel with an N-15 nuclear resonance

J.-S. Larochelle, A. Désilets-Benoit, E. Martel, G. Borduas, S. Roorda

sjoerd.roorda@umontreal.ca

Département de physique, Université de Montréal, Pavillon Roger-Gaudry, Case postale 6128, succursale Centre-ville, Montréal (Québec), H3C 3J7, Canada

We have used a 6.385 MeV ^{15}N nuclear resonance to detect hydrogen in steel that had been electroplated with a protective Cd surface coating to better understand the parameters leading to hydrogen embrittlement. The narrow energy range of the nuclear reaction allows a high depth precision within a total depth of 2 micron while the high cross section yields a high signal to noise ratio [1,2].

At room temperature we observe a rapid decline in hydrogen concentration during the measurement, indicative of beam-induced hydrogen detrapping and mobility [3,4]. It appears that the hydrogen concentration falls off as a simple exponential decay with ion fluence, however it settles at a finite hydrogen concentration different from 0. In spite of the hydrogen loss, we have been able to detect small concentrations of hydrogen which has diffused into the bulk of the steel sample. We also looked at the system at liquid nitrogen temperature to observe in more detail the temperature dependence and asymptotic behaviour of the hydrogen loss and will report on these studies.

[1] P. Trocellier and C. Englemann, “Hydrogen depth profile measurement using resonant nuclear reaction : an overview”, *Journal of Radioanalytical and Nuclear Chemistry*, vol 100, No 1, pp. 117-127, 1985

[2] M. Castellote et al., “Hydrogen embrittlement of high-strength steel submited to slow strain rate testing studied by nuclear resonance reaction analisys and neutron diffraction”, *Nuclear Instruments and Methods in Physics Research, Section B : Beam Interactions with Materials and Atoms*, vol. 259, No 2, pp. 975-983, 2007

[3] B. Pantchev, P. Danesh, B. Schmidt, D. Grambole and W. Möller, “Ion beam-induced hydrogen migration in SiO2/a-Si:H/SiO2 layer stack”, *Semiconductor Science and Technology*, Vol 24, No 3, 035012, 2009

[4] K. Takeyasu, M. Matsumoto and F. Fukutani, “Temperature dependance of hydrogen depth distribution in the near-surface region of stainless steel”, *Vacuum*, vol. 109, pp. 230-233, 2014

Element, valence and orbital depth profiling with resonant x-ray reflectometry

R.J. Green[1,2,3], S. Macke[1,2,4], and G.A. Sawatzky[1,2]

rgreen@phas.ubc.ca

[1]*Quantum Matter Institute, University of British Columbia, Vancouver, Canada V6T 1Z4*
[2]*Department of Physics & Astronomy, University of British Columbia, Vancouver, Canada V6T 1Z1*
[3]*Max Planck Institute for Chemical Physics of Solids, Nöthnitzerstraße 40, 01187 Dresden, Germany*
[4]*Max Planck Institute for Solid State Research, Heisenbergstraße 1, 70569 Stuttgart, Germany*

Spurred by advances in atomic-precision film growth, oxide heterostructures have become a very active field of study in recent years. The interfaces in such heterostructures exhibit a wide range of emergent phenomena, such as interface charge transfer, two dimensional electron liquids, superconductivity, and ferromagnetism between non-magnetic materials [1]. Such phenomena result from the interface-induced tuning of the various spin, charge, orbital, and lattice degrees of freedom, and show great promise for electronics applications. However, while the emergent properties are readily apparent, obtaining electronic structure information specific to the nanometer-scale buried interface region—in order to understand and further tune the these properties—is an understandably difficult task.

In this talk I will present our studies of the interfacial and depth dependent electronic structure of heterostructures using resonant x-ray reflectometry (RXR), a new experimental technique which combines the powerful electronic structure probing capability of x-ray absorption spectroscopy with the interface and depth sensitivity provided by quantitative reflectometry. By tuning our x-ray experiment to various different reflection geometries and resonance energies, we can obtain information on the depth-dependent, element-specific electronic structure directly at and near buried interfaces. For the paradigmatic $LaAlO_3/SrTiO_3$ heterostructure which exhibits orbital and electronic reconstructions [2,3], we extract atomic layer-resolved, reconstructed Ti orbital energies within a few unit cells of the interface, and determine the depth profile of the charge in the interfacial 2D electron liquid. These results provide important insight into physics behind the intriguing emergent phenomena, and show RXR to be an ideal tool for studying oxide interfaces.

References.

[1] Emergent phenomena at oxide interfaces. Hwang et al., *Nature Mater.* 11 (2012) 103.
[2] A high-mobility electron gas at the $LaAlO_3/SrTiO_3$ heterointerface. A. Ohtomo and H. Y. Hwang, *Nature* 427 (2004) 423.
[3] Orbital reconstruction and the two-dimensional electron gas at the $LaAlO_3/SrTiO_3$ interface. M. Salluzzo et al., *Phys. Rev. Lett.* 102 (2009) 166804.

19

Transmission SIMS: A novel approach to achieving higher secondary ion yields of intact biomolecules

K. Nakajima[1], K. Nagano[1], T. Marumo[1], K. Yamamoto[1], K. Narumi[2], Y. Saitoh[2], K. Hirata[3], **K. Kimura**[1]

kimura@kues.kyoto-u.ac.jp

[1] Department of Micro Engineering, Kyoto University, Kyoto 615-8540, Japan;
[2] Takasaki Advanced Radiation Research Institute, QST, Takasaki, Gumma 370-1292, Japan;
[3] National Metrology Institute of Japan, AIST, 1-1-1 Higashi, Tsukuba, Ibaraki 305-8565, Japan;

There has been an increasing demand to extend accessible mass range in secondary ion mass spectrometry (SIMS) particularly for biological and biomedical molecular imaging. During the past two decades, various kinds of large cluster ions, such as C_{60} ions, argon gas cluster ions, water cluster ions, and metal cluster ions have been used as primary ions. It was shown that these cluster ions enhance emission of intact large molecular ions compared to monatomic ion bombardment. In SIMS, secondary ions emitted from a sample in the backward direction with respect to the incident direction of the primary ion are usually measured. If the sample is a self-supporting thin film, the secondary ions emitted in the forward direction upon transmission of the primary ions can be also measured. So far, there have been only few studies about the transmission SIMS. Boussofiane-Baudin *et al* found small enhancement of the secondary ion yield in the forward direction compared to the backward direction [1]. The origin of the enhancement was suggested to be the larger stopping power at the exit surface due to higher charge states achieved during the passage through the sample film. In this presentation, we demonstrate that large enhancement of the secondary ion yield of intact biomolecules can be achieved by combining the cluster ions (5 MeV C_{60}^+) with the transmission SIMS. We measured secondary ions emitted in the forward direction from phenylalanine amino acid films deposited on self-supporting amorphous Si_3N_4 (a-SiN) films. We found significant enhancement of the intact phenylalanine ion yield and large suppression of fragment ions compared to the backward direction [2].

Phenylalanine amino acid was purchased from Nakalai Tesque (Japan) and used without further purification. Self-supporting a-SiN films (1.5×1.5 mm^2) of thickness 20 – 50 nm were purchased from Silson Ltd (Northampton, UK). Thin films of phenylalanine (20 – 100 nm) were deposited on the a-SiN films using vacuum evaporation. The thickness and uniformity of the deposited phenylalanine films were examined by measuring energy loss spectra of 6 MeV Cu^{4+} ions passing through the phenylalanine/a-SiN films. A beam of 5 MeV C_{60}^+ ions was produced by a 3MV tandem accelerator at QST/Takasaki. The beam was collimated by an aperture (diameter 1mm) and sent to a scattering chamber (base pressure 1×10^{-6} Pa). For the SIMS measurements, the beam current was reduced to less than 0.1 fA. The collimated beam was incident on the phenylalanine/a-SiN film from the a-SiN side at 45° with respect to the surface normal. Mass spectra of secondary ions emitted in the forward direction were measured by a time-of-flight setup. We also measured the secondary ions emitted in the backward direction from the phenylalanine film using the same equipment.

Figure 1 shows the observed mass spectra of positive secondary ions emitted in the forward (solid line) and backward (dashed line) directions observed using 5 MeV C_{60}^+ ions. A peak of protonated intact phenylalanine ions $[Phe+H]^+$ is seen at m/z = 166. There are also many peaks corresponding to fragment ions, for example, $[Phe-COOH]^+$ ions at m/z = 120, $C_8H_8^+$ ions at m/z = 104, $C_7H_7^+$ ions at m/z = 91, $C_6H_5^+$ ions at m/z = 77, and so on. Both spectra

are similar but the yield of the intact phenylalanine ion is enhanced in the forward direction compared to the backward direction by a factor of 8. Similar enhancement is also seen for the large fragment ions, *e.g.* the yield of $[Phe\text{-}COOH]^+$ is enhanced by a factor of 4. For smaller fragment ions, however, the yield is reduced in the forward direction compared to the backward. The origin of these behaviors is attributed to a broader spatial distribution of constituent carbon ions at the exit surface due to the multiple scattering during the passage through the sample film. In the present case, FWHM of the distribution is estimated to be ~ 50 nm using the SRIM code, which is about 70 times larger than the diameter of C_{60}^+. As a result, the distribution of the deposited energy is broader with a lower peak energy density at the exit surface. Such a distribution is preferable for the soft ionization which enhance the yield of intact molecular ions and suppress fragmentation.

The authors are grateful to the crew of the 3 MV tandem accelerator at QST/Takasaki for providing the 5 MeV C_{60}^+ beam. This work was partly supported by JSPS KAKENHI Grant (Grant Number 26246025).

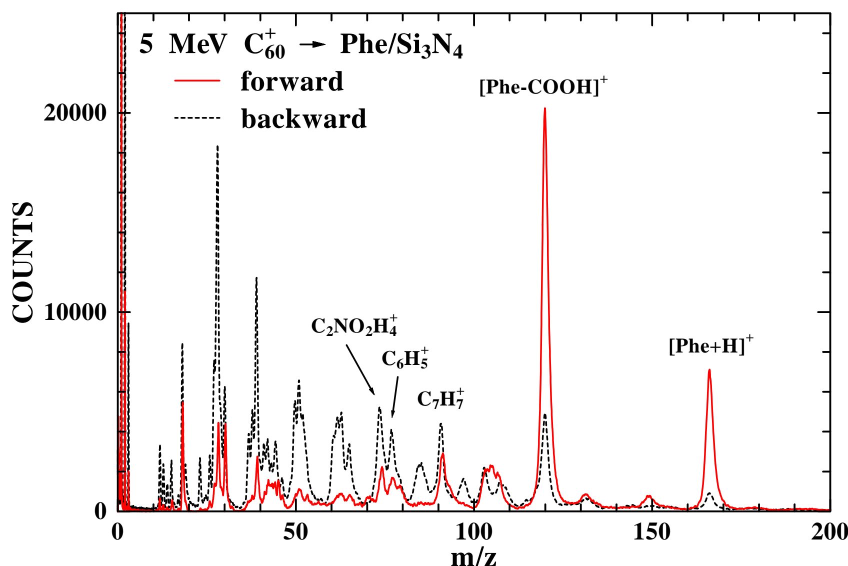

Figure 1. Mass spectra for positive secondary ions from phenylalanine/a-SiN films under 5 MeV C_{60}^+ ion bombardment. The spectra observed in the forward direction (solid line) and the backward direction (dashed line) are shown.

References

[1] K. Boussofiance-Baudin, A. Brunelle, P. Chaurand, S. Della-Negra, J. Depauw, P. Hakansson and Y.Le Beyec, Nucl. Instr. and Methods in Phys. Res. B, **88** (1994) 61.

[2] K. Nakajima, K. Nagano, M. Suzuki, K. Narumi, Y. Saitoh, K. Hirata, and K. Kimura, Appl. Phys. Lett. **104** (2014) 114103.

20

Investigation of electric double layer at liquid interface with TOF-MEIS

H.J. Kim, K.W. Chung, **D.W. Moon**

dwmoon@dgist.ac.kr

Department of New Biology, DGIST, TechnoDaeRo 333, Dalsung, Daegu, Korea 711-873

The presence of electric double layer (EDL) at liquid interface has been recognized for last 100 years but the atomic scale structure of EDL has not been revealed, even though optical or electrical techniques could monitor the change of EDL. Most of atomic scale surface and interface analysis techniques are based on vacuum so that liquid interfaces can be hardly investigated.

We designed an ultra high vacuum compatible liquid cell with a single layer graphene window so that MEIS analysis can be applied to the graphene liquid interface. We clearly observed the EDL structure formed between CuO and KI solution showing I accumulation and K depletion at the EDL with the width of ~1 nm.

Studies on systematic dependence of EDL structure on the bias voltage and electrolyte concentration are in progress. Preliminary results on EDL structure profiling and further prospective on bio-liquid interface, protein adsorption, and artificial cell membrane structure will be reported for discussions and comments

21

Multiple scattering and geometry effects on depth profiling of 2D and 3D structures

F. Schiettekatte

francois.schiettekatte@umontreal.ca

Regroupement Québécois sur les Matériaux de Pointe (RQMP), Département de physique, Université de Montréal, Montréal, Québec, Canada, H3C 3J7

High-resolution ion beam depth profiling often involves using beam at medium or low energy, or using heavy ions with high stopping power. In both cases, multiple scattering (MS) becomes an important effect, which affects depth resolution in way that is not always easy to model. For example, in the case of grazing incidence or detection, the effect of MS becomes asymmetric as the fraction of the particles that are on one side of the trajectory can quit the sample surface. At deeper depth, large angle MS becomes a prominent effect that affects the spectrum background and peak shape in a peculiar way.

In this presentation, we report on how, in the case of 2D or 3D structures, the MS effects combined to the fact that detectors have a finite size also affect the spectrum shape. For this purpose, the latest version of Corteo [1,2], a Monte Carlo (MC) simulation code for ion beam analysis is presented. This version simulates the trajectory of ions in targets described by a pixel or voxel image of arbitrary size, during which the detailed trajectory of each ion is simulated. In simulations of samples with 2D or 3D structures parallel to the beam axis, a fraction of the ions escape the walls of the structures due to MS. Since the MS effect increases with depth, the effect is non-uniform as a function of depth. Also, the shape of the spectrum is influenced by the fact that, when considering a detector with a finite size (rather than a point detector often considered in analysitcal simulations), the ions that escaped the wall of a 2D/3D structure can still reach the detector. Other effects such as re-entry, outlined by MC simulations, are also presented.

References

[1] Fast Monte Carlo for Ion Beam Analysis Simulations. F. Schiettekatte, Nucl. Instrum. Meth. B 266 (2008) 1880.

[2] Spectrum simulation of rough and nanostructured targets from their 2D and 3D image by Monte Carlo methods. F. Schiettekatte, M. Chicoine, Nucl. Instrum. Meth. B 371 (2016) 106.

22

3-D atom-by-atom dissection of materials

O. Moutanabbir

Department of Engineering Physics, École Polytechnique de Montréal

oussama.moutanabbir@polymtl.ca

After a long gestation period, atom-probe tomography (APT) is finally coming of age. The availability of reliable and well-engineered commercial instruments and data analysis software has meant that APT is now being applied to a broad range of materials, including oxides, organic/inorganic interfaces, and biological materials, as well as metals and semiconductors. In this presentation, I will describe the underlying physics of laser-assisted field evaporation which is the cornerstone of APT analysis. I will also describe the science and practice of its use to achieve 3-D atom-by-atom maps of different materials including nanoscale metal-semiconductor interfaces and isotopically engineered quantum materials.

Beta-detected Nuclear Magnetic Resonance (β-NMR): Towards depth resolved NMR

V.L. Karner[1], R.M.L. McFadden[1], A. Chatzichristos[2], D. Fujimoto[2], I. McKenzie[4], G.D. Morris[4], D.L. Cortie[5], R.F. Kiefl[2], W.A. MacFarlane[1,3]

wam@chem.ubc.ca

[1]*Department of Chemistry, University of British Columbia, Vancouver, BC, Canada*
[2]*Department of Physics and Astronomy, University of British Columbia, Vancouver, BC, Canada*
[3]*Stewart Blusson Quantum Matter Institute, 2355 East Mall, Vancouver, BC V6T 1Z4, Canada*
[4]*TRIUMF, 4004 Wesbrook Mall, Vancouver, BC V6T 1Z4, Canada*
[5]*College of Physical and Mathematical Sciences, Australian National University, Canberra ACT 2601, Australia*

Nuclear magnetic resonance (NMR) spectroscopy is a powerful technique in chemistry and condensed matter physics. It is non-destructive, non-perturbative, and can analyze a large variety of samples. However it requires large sample sizes (~1 g), it is a bulk technique, and there is an intrinsically small signal-to-noise ratio. Beta-detected NMR is a twist on conventional NMR, in which the signal is measured by the beta decay of a polarized, radioactive ion. In β-NMR a low energy ion beam (0.1-30 keV) is implanted into the sample of interest, and the asymmetry in the beta decay of the ion is measured. The most common isotope used is ^{8}Li, which has a half-life of 848 ms, and spin $I=2$ [1].

Our group uses the β-NMR facility at TRIUMF in Vancouver. At TRIUMF, the ISAC facility produces beams of short-lived radioisotopes for research in nuclear physics and materials science. For Li, a surface ionization source can routinely produce high quality beams of intensity ~10^7/s with typical transport energy of 20 keV. The ion beam can be electrostatically decelerated at the spectrometer end station, allowing depth-resolved NMR measurements in the range 2 to 200 nm. Using this technique our group has investigated a variety of samples; which include thin films, heterostructures, and crystals [2,3,4,5,6,7].

Although we have been successful in doing depth resolved β-NMR measurements for certain samples, the technique is inherently limited, at the lowest implantation energies (< 2 keV), by a background signal due to backscattered ions. Knowledge of the implantation profile is a key input for a quantitative interpretation of depth dependent phenomena. Typically the profiles are calculated using TRIM [8]. This is reasonable in many cases, but in some cases it is not sufficient, for example, when channeling is important.

References

[1] Implanted-ion β-NMR: A new probe for nanoscience. W.A. MacFarlane. Solid State Nucl. Magn. Reson. 68-69 (2015), 1-12.

[2] Depth dependence of the structural phase transition of $SrTiO_3$ studied with β-NMR and grazing incidence x-ray diffraction. Z. Salman, M. Smadella, W.A. MacFarlane, B.D. Patterson, P.R. Willmot, K.H. Chow, M.D. Hossain, H. Saadaoui, D. Wang, R.F. Kiefl. Phys. Rev. B. 83 (2011), 224112.

[3] Hyperfine fields in an Ag/Fe multilayer film investigated with ^{8}Li β-detected nuclear magnetic resonance. T.A. Keeler, Z. Salman, K.H. Chow, B. Heinrich, M.D. Hossain, B. Kardasz, R.F. Kiefl, S.R. Kreitzman, W.A. MacFarlane, O. Monsendz, T.J. Parolin, D. Wang. Phys. Rev. B. 77 (2008), 144429.

[4] β-detected NMR of Li in $Ga_{1-x}Mn_xAs$. Q. Song, K.H. Chow, Z. Salman, H. Saadaoui, M.D. Hossain, R.F. Kiefl, C.D.P. Levy, M.R. Pearson, T.J. Parolin, M. Smadella, D. Wang, K.M. Yu, X. Liu, J.K. Furdyna, W.A. MacFarlane. Phys. Rev. B. 84 (2011), 054414.

[5] Finite-size effects in the nuclear magnetic resonance of epitaxial palladium thin films. W.A. MacFarlane, T.J. Parolin, T.I. Larkin, G. Richter, K.H. Chow, M.D. Hossain, R.F. Kiefl, C.D.P. Levy, G.D. Morris, O. Ofer, M.R. Pearson, H. Saadaoui, Q. Song, D. Wang. Phys. Rev. B. 88 (2013), 144424.

[6] Enhanced high-frequency molecular dynamics in the near-surface region of polystyrene thin films observed with β-NMR. I. McKenzie, C.R. Daley, R.F. Kiefl, C.D. Levy, W.A. MacFarlane, G.D. Morris, M.R. Pearson, D. Wang, J.A. Forrest. Soft Matter 11 (2015), 1755.

[7] β-NMR investigation of the depth-dependent magnetic properties of an antiferromagnetic surface. D.L. Cortie, T. Buck, M.H. Dehn, V.L. Karner, R.F. Kiefl, C.D.P. Levy, R.M.L. McFadden, G.D. Morris, I. McKenzie, M.R. Pearson, X.L. Wang, W.A. MacFarlane. Phys. Rev. Lett. 116 (2016), 106103.

[8] Particle interactions of ions with matter. J.F. Ziegler. http://www.srim.org/

24

MEIS regained at the IIAA in Huddersfield University

J.A. van den Berg, A.K. Rossall, P. Bailey and R.J. Barlow

j.vandenberg@hud.ac.uk

International Institute for Accelerator Applications (IIAA), School of Computing and Engineering, University of Huddersfield, Huddersfield, HD1 3DH, UK.

The UK Medium Energy Ion Scattering (MEIS) facility operated at Daresbury Laboratory from 1996 until 2011 during which time it was used by some 30 UK and overseas research groups. Due to its integral surface science station the MEIS facility was used for a broad range of fundamental and applied science experiments and this, in turn, led to a high level of publications, typically one per month during the last four years of its funded operation and contributed significantly to the training of PhD students and researchers.

A year after funding for the MEIS facility terminated, the newly set up International Institute for Accelerator Applications (IIAA) at the University of Huddersfield offered the MEIS equipment a new home. Reconstruction of the MEIS end station including its surface science analytical chamber commenced in mid 2012. Since many of the beamline components, due to their previous use had low level radioactive contamination and could not be reused, a completely new 200 keV ion beamline was constructed at the IIAA. Using mainly existing components gathered from different sources, a simpler beamline design was implemented and fitted with a much less complex control system. Its eventual operation has proved to be remarkably stable and reliable. The rebuilt MEIS facility is schematically shown below.

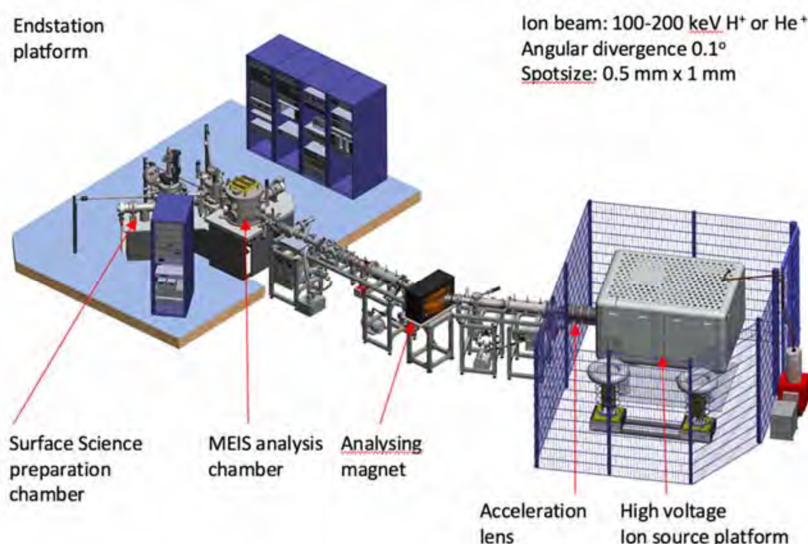

With its unique capability of being able to yield both structural and compositional information on surfaces e.g. adatom position or overlayer registry and high resolution depth profiling of nanolayers, MEIS continues to take in a key niche in the world of materials science and engineering. Aspects of the new MEIS facility and its reconstruction process will be presented as will some fundamental points of MEIS including quantification as well as examples of recent studies using the IIAA MEIS facility mainly in the area of depth profiling analysis (high-k nano-layers, plasma doping). The facility is open for collaborative research projects.

Electronic stopping of slow protons in oxides

D. Roth[1], B. Bruckner[1], A. Mardare[2], Ch.L. McGahan[3], M. Dosmailov[4], J.I. Juaristi[5,6,7], M. Alducin[5,6], D. Primetzhofer[8], R.F. Haglund, Jr.[3], J.D. Pedarnig[4], and P. Bauer[1,6]

dietmar.roth@jku.at

[1]Institut für Experimentalphysik, Johannes Kepler Universität Linz, Altenbergerstraße 69, A-4040 Linz, Austria
[2]Institut für Chemische Technologie Anorganischer Stoffe, Johannes Kepler Universität Linz, Altenbergerstraße 69, A-4040 Linz, Austria
[3]Department of Physics and Astronomy and Interdisciplinary Materials Science Program, Vanderbilt University, Nashville, Tennessee 37235-1807, USA
[4]Institut für Angewandte Physik, Johannes Kepler Universität Linz, Altenbergerstraße 69, A-4040 Linz, Austria
[5]Centro de Física de Materiales CFM/MPC (CSIC-UPV/EHU), P. Manuel de Lardizabal 5, 20018 Donostia-San Sebastián, Spain
[6]Donostia International Physics Center DIPC, P. Manuel de Lardizabal 4, 20018 San Sebastián, Spain
[7]Departamento de Física de Materiales, Facultad de Químicas, Universidad del País Vasco (UPV/EHU), Apartado 1072, 20018 San Sebastián, Spain
[8]Institutionen för Fysik och Astronomi, Uppsala Universitet, Box 516, S-751 20 Uppsala, Sweden

The energy loss of ions in matter has been under close investigation for many decades. In this field of research, profound knowledge about ion-target interactions is obtained. Data on the deceleration of ions in solids are useful in many fields like material science (ion beam analytics) or medicine (radiation therapy).

Kinetic energy of the projectile is transferred to the target due to two distinct processes: either by repulsive Coulomb interaction with the nuclei (nuclear stopping) or by excitation of electrons (electronic stopping). The mean energy loss per path length due to interaction with electrons is given by the electronic stopping power $S = dE/dx$. In order to eliminate the density dependence of S, often the electronic stopping cross section $\varepsilon = 1/n\, S$ is used, where n denotes the atomic density. While in the area of high energy ions (~ MeV energy) the behavior of the electronic stopping power is well understood for many materials, there still persist many unanswered questions for low energy ions (~ keV energy).

In the regime of low-energy ion scattering (LEIS), i.e. for primary ion energies from 0.5 to 10 keV, theory predicts that for a free electron gas (FEG) $S \propto v$, if the projectile velocity v is sufficiently low compared to the Fermi velocity v_F of the target electrons [1, 2]. The linear velocity dependence has been found also experimentally for protons in a FEG-like metal, as e.g. Al, [3, 4]. However, it has been shown that the band structure of the sample can strongly alter the velocity dependence of S: for noble metals like Cu, Ag or Au S shows a change in its velocity dependence correlated with the excitation of *d*-band electrons, located several eV below the Fermi energy [5, 6, 7]. For large band gap materials, e.g., KCl and LiF, electronic energy loss vanishes for ions slower than a certain threshold velocity v_{th} [8, 9]. A comparison to a TD-DFT calculation of electronic stopping of H^+ in LiF [10] shows that the experimental value of v_{th} is lower by a factor of 2. This suggests that for ionic crystals there may exist different energy loss channels in addition to electron-hole pair excitation. In order to close the gap between metals and insulators, oxides are perfect candidates: they feature band gaps of different sizes giving rise to either semiconducting or insulating properties.

In this contribution, we present low-velocity electronic stopping cross sections of protons in ZnO, VO_2, Ta_2O_5 and HfO_2. In case of VO_2, electronic stopping was measured in both, the semiconducting and the metallic phase (above 67 °C sample temperature). The results are

compared to earlier measurements of SiO_2 [8] and Al_2O_3 [11]. This selection permits to evaluate the electronic energy loss of oxides featuring band gaps between 0 eV (VO_2 in metallic phase) and ~ 9 eV (SiO_2). In order to look how the band structure is correlated with the electronic energy loss, DFT calculations of the electronic density of states (DOS) were performed.

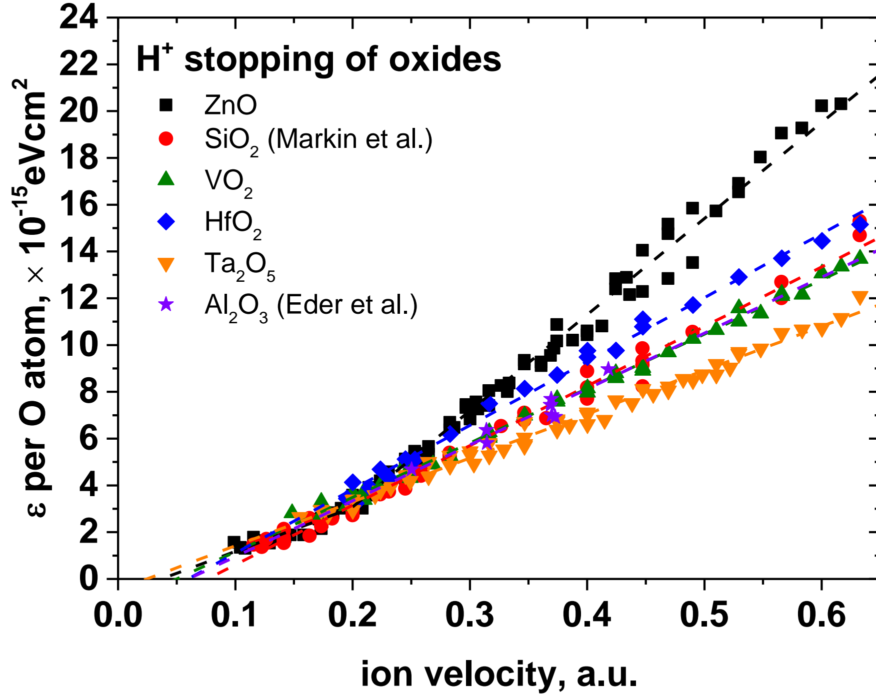

Fig. 1: H^+ electronic stopping cross sections per O atom of ZnO, SiO_2, VO_2, HfO_2, Al_2O_3 and Ta_2O_5 are shown as a function of ion velocity in atomic units. At very low ion velocities (v< 0.5 a.u.) electronic energy loss in all oxides coincides in efficiency.

For oxides it seems reasonable to characterize the stopping behavior in terms of ε per molecule, since the molecule comprises all valence electrons. To compare the stopping efficiency for the same number of valence electrons, it makes sense to divide the ε per molecule by the abundance of O in the molecule. In Fig. 1 this quantity is presented for ZnO, SiO_2, VO_2, HfO_2, Al_2O_3 and Ta_2O_5 as a function of the ion velocity in atomic units v/v_0, where $v_0 = c/137$ is the Bohr velocity. At $v < 0.25$ a.u., i.e., for $E < 1.5$ keV, for all oxides the electronic stopping cross sections per oxygen atom coincide. At $v > 0.25$ a.u. the electronic stopping cross sections of most oxides match within 10 %, with the exception of ZnO, where the contribution from *d*-band excitation results in a higher ε.

We will discuss to what extent properties like valence electron density (plasmon energy), electronic structure, band gap or effects like perturbation of the band structure by the ion (metallization) influence electronic stopping of protons in oxides.

References.

[1] R.H. Ritchie. Phys. Rev. 114, 3 (1959). pp 644-654.
[2] P.M. Echenique, R.M. Nieminen, J.C: Ashley, and R.H. Ritchie. Phys. Rev. A 33 (1986), 897.
[3] J.E. Valdés, G. Martínez Tamayo, G.H. Lantschner, J.C. Eckardt and N.R. Arista, Nucl. Instr. And Meth. B 73 (1993). pp 313-318.
[4] D. Primetzhofer, S. Rund, D. Roth, D. Goebl, and P. Bauer. Phys. Rev. Lett. 107 (2010), 163201.
[5] S.N. Markin, D. Primetzhofer, M. Spitz and P. Bauer. Phys. Rev. B 80, 205105 (2009).

[6] J.E. Valdés, J.C. Eckardt, G.H. Lantschner and N.R. Arista. Phys. Rev. A 49, 2 (1994). pp 1083-1088.
[7] M.A. Zeb, J. Kohanoff, D. Sánchez-Portal, A. Arnau, J.I. Juaristi, and E. Artacho. Phys Rev. Lett. 108 (2012), 225504.
[8] S.N. Markin, D. Primetzhofer and P. Bauer. Phys. Rev. Lett. 103 (2009), 113201.
[9] L.N. Serkovic Loli, E.A. Sánchez, O Grizzi and N.R. Arista. Phys. Rev. A 81 (2010), 022902.
[10] J.M. Pruneda, D. Sánchez-Portal, A. Arnau, J.I. Juaristi, and E. Artacho. Phys. Rev. Lett. 99 (2007), 235501.
[11] K. Eder, D. Semrad, P. Bauer, P. Maier-Komor, F. Aumayr, M. Peñalba, A. Arnau, J.M. Ugalde, and P.M. Echenique. Phys. Rev. Lett. 79 (1997), 4112.

Interface strain study of ultra-thin HfO_2 films on Ge and GeSn substrates using HR-RBS

S.K. Vajandar[1], W. Wang[2], T.K. Chan[1], E.S. Tok[1], Y.C. Yeo[2], T. Osipowicz[1]

phyto@nus.edu.sg

[1] Centre for Ion Beam Applications (CIBA), Department of Physics, National University of Singapore, Singapore 117551

[2] Department of Electrical and Computer Engineering, National University of Singapore, Singapore 117576

Strain depth profiling has been performed and studied in ultra-thin HfO_2 (3.8nm) films deposited on Ge (001) and $Ge_{0.92}Sn_{0.08}$ (001) substrates using high-resolution Rutherford backscattering spectroscopy in combination with angular channeling scans. Furthermore, interface quality and substrate crystal quality were determined for these samples. Both Ge and GeSn have been studied extensively in recent years as they are candidates for the replacement of Si in high-speed and low-power microelectronic devices. GeSn compounds are promising because of their large carrier mobility and the possibility for direct bandgap semiconductor formation. HfO_2 is utilized as a high-k dielectric in Si technology, and investigated as an alternative dielectric for GeSn substrates. Therefore, quantitative analysis of the interface quality and the lattice strain in HfO_2/Ge and HfO_2/GeSn may be of critical importance, because these properties will determine electrical properties in devices.

A MEIS, STM and RAIRS investigation of the adsorption of CO on cobalt/palladium bimetallic surfaces

A. Murdoch[1], A.G. Trant[1], J. Gustafson[1*], T.E. Jones[1], T.C.Q. Noakes[2], P. Bailey[2] and **C.J. Baddeley**[1]

cjb14@st-andrews.ac.uk

[1] EaStCHEM School of Chemistry, University of St Andrews, St Andrews, Fife, KY169ST, United Kingdom
[2]. MEIS facility, STFC Daresbury Laboratory, Daresbury, Cheshire, WA44AD, United Kingdom
** Present address: Div. of Synchrotron Radiation Research, Lund University, Box 118, 22100 Lund, Sweden*

Bimetallic catalysts often outperform their monometallic analogues both in terms of their activity and selectivity [1]. There are many examples of industrial heterogeneous catalysts whose active component consists of bimetallic nanoparticles. Fischer-Tropsch (FT) catalysis is used to convert syngas (CO/H_2 mixtures) into hydrocarbon products. Cobalt is one of the most important metals for FT catalysis and the addition of palladium has been shown to enhance the catalytic performance of cobalt catalysts [2]. Establishing the composition of bimetallic surfaces in the presence of the reactive gas phase is an important step towards understanding the promoting effect of the second metal on a catalytic reaction. The unique depth profiling capabilities of medium energy ion scattering (MEIS) are highly suited to characterising the phenomenon of adsorbate induced segregation [3,4]. We report an investigation of the growth and annealing behaviour of ultrathin Co films on Pd{111} using MEIS, low energy electron diffraction (LEED) and scanning tunnelling microscopy (STM). Incremental annealing of Co/Pd{111} results in intermixing and the formation of an ordered CoPd alloy at 560 K. Under these conditions, MEIS reveals that the top three layers consist of an approximately equimolar mixture of Co and Pd. STM and LEED provide evidence that the overlayer has a p(2×1) registry leading to the conclusion that the surface is terminated in the {111} plane of the CoPd $L1_0$ structure [5]. In addition, we report the adsorption of CO onto bimetallic CoPd surfaces on Pd{111} using a combination of reflection absorption infrared spectroscopy (RAIRS) and MEIS. The vibrational frequency of adsorbed CO provides crucial information on the adsorption sites adopted by CO and MEIS probes the surface composition before and after CO exposure. We show that cobalt segregation is induced by CO adsorption and rationalise these observations in terms of the strength of adsorption of CO in various surface adsorption sites [6].

References.

[1] Structure of bimetallic clusters. J. H. Sinfelt. Acc. Chem. Res. 20 (1987) 134-139
[2] CO hydrogenation and methane activation over Pd-Co/SiO_2 catalysts prepared by sol/gel method. L. Guczi, L. Borko, Z. Schay, D. Bazin and F. Mizukami. Catal. Today 65 (2001) 51-57.
[3] Oxidation-induced segregation at the $Pt_{0.5}Ni_{0.5}$(111) surface studied by MEIS. S. Deckers, F. Habraken, W. F. van der Weg, A. W. D. van der Gon, J. F. van der Ween and J. W. Geus Appl. Surf. Sci. 45 (1990) 121-129
[4] Quantitative analysis of adsorbate induced segregation at bimetallic surfaces: Improving the accuracy of MEIS results. C. J. Baddeley, L. H. Bloxham, S. C. Laroze, R. Raval, T. C. Q. Noakes and P. Bailey. J. Phys. Chem. B 105 (2001) 2766-2772
[5] Alloy formation in the Co/Pd{111} system - A study with MEIS and STM. A. Murdoch, A. G. Trant, J. Gustafson, T. E. Jones, T. C. Q. Noakes, P. Bailey and C. J. Baddeley. Surf. Sci. 608 (2013) 212-219
[6] The influence of CO adsorption on the surface composition of cobalt/palladium alloys. A. Murdoch, A. G. Trant, J. Gustafson, T. E. Jones, T. C. Q. Noakes, P. Bailey and C. J. Baddeley. Surf. Sci. 646 (2016) 31-36

Neutron reflectometry as *in situ* probe of thin film composition and layer structure for investigating corrosion and hydrogen absorption in titanium

J.J. Noël[1], Z. Tun[2], and D.W. Shoesmith[1]

jjnoel@uwo.ca

[1]Department of Chemistry, The University of Western Ontario
London, ON Canada N6A 5B7
[2]Canadian Neutron Beam Centre, National Research Council of Canada, Chalk River, ON Canada, K0J 1J0

Titanium readily absorbs hydrogen into its lattice in solid solution, and precipitates crystals of a separate hydride (TiH_x) phase once the local concentration of dissolved hydrogen atoms reaches or exceeds the solubility limit. The presence of a hydride phase in Ti tends to make the material more brittle, leading eventually to brittle fracture under tensile stress, in the form of hydrogen-induced cracking (HIC). Adsorbed hydrogen atoms can be generated on Ti surfaces by cathodic polarization or as a by-product of the corrosion reaction, under certain conditions, and these hydrogen atoms in some circumstances, can be a source of absorbed hydrogen in the material. Fortunately, Ti surfaces exposed to air or aqueous environments tend to be covered by an extremely adherent and highly insoluble TiO_2 film that acts as a very good barrier to both corrosion and hydrogen absorption.

This presentation describes the use of in situ neutron reflectometry measurements to follow the growth of the protective oxide film on Ti under anodic polarization in 0.27 M NaCl solution and the subsequent defeat of this oxide barrier under cathodic polarization, leading to hydrogen ingress and mechanical failure. In neutron reflectometry, a ribbon beam of monochromatic thermal neutrons is elastically scattered from the flat surfaces (outermost or buried) within a sample. The intensity of elastic scattering (i.e., reflectivity) and its variation with the scattering vector (a function of incidence angle) allow the determination of the composition and thickness of any surface layers, in situ and non-destructively, with a resolution of about 1 at.% and 0.5 nm, to a maximum thickness of about 300 nm. Neutrons are also uniquely sensitive to hydrogen and readily differentiate between hydrogen (^1H) and deuterium (^2H).

Our experiments demonstrated the incorporation of OH species from water during the anodic growth of the oxide film on Ti, the validity of the anodization and Pilling-Bedworth ratios for Ti measured by other means, and tracked the progress of electrochemically introduced absorbed hydrogen as it penetrated the oxide film and entered and eventually destroyed a thin Ti film on Si substrate.

Vacancy-impurity interactions in ion-implanted silicon

P.J. Simpson[1], J. Rideout[2], A.P. Knights[2]
psimpson@uwo.ca

[1] The University of Western Ontario, Department of Physics and Astronomy, London, Ontario N6A 3K7
[2] McMaster University, Department of Engineering Physics, Hamilton, Ontario L8S 4L8

We have investigated the role of impurities in the annealing of ion-implanted silicon. The process of ion implantation creates vacancies and interstitials, as well as introducing impurities. These populations interact with impurities already present in the host material, especially oxygen and dopant species. In order to explore the energetics of defect migration, we have constructed a positron accelerator to probe vacancy-type defects via positron annihilation, with an *in situ* gas-source ion implanter. This novel apparatus allows us to implant energetic ions at cryogenic temperatures, and to probe vacancy concentrations as a function of isothermal annealing time and temperature. The dependence of annealing behaviour on impurity concentrations in the starting material provides a window into vacancy-impurity interactions that are important to the doping of silicon devices.

ABSTRACTS POSTER

Medium energy ion scattering and elastic recoil detection for solar silicon devices

M. Brocklebank[1], L.V. Goncharova,[1] D. Barchet,[2] N.P. Kherani[2]

lgonchar@uwo.ca

[1]Department of Physics and Astronomy, Western University, London, ON, Canada.
[2] Department of Electrical & Computer Engineering, University of Toronto, Toronto, ON, M5S 3G4, Canada

Significant enhancement of silicon-based devices reliability (lifetime) has been observed with the quality of the surface passivation. The standard thermal oxide growth involves processing at temperatures above 800ºC, which can degrade crystalline Si properties, via defect and dopants migration, and segregation processes at the interface, lowering device lifetime. In order to overcome this obstacle, novel passivation was proposed that can be implemented at low temperatures.[1] In addition, some of the lifetime enhancements were contributed to hydrogen present at the SiO_2/Si interface.[2] The effect has been attributed to reduced hot-election depassivation of hydrogenated and deuterated SiO_2/Si interfaces, where H or D passivates silicon dangling bonds. Possible mechanisms explaining this behaviour is the coupling of Si-H vibrational bending mode to bulk phonons in crystalline silicon.[3] It is undoubtedly a great advantage to be able to properly characterize not only bulk properties of Si devices but in addition, to provide determination of the precise character of any interfaces with high depth resolution and element sensitivity. Such insight into the bulk or surface properties can be related back to things like device performance or provide insight into why a particular material has the properties it does.

In this work we explore interface properties of crystalline Si heterojunction solar cells with plasma enhanced chemical vapour deposition (PECVD) grown silicon nitride layers with efficiencies approaching 17%.[1] The role of hydrogen at the interface was evaluated using elastic recoil detection (ERD), while interface profiling was done by medium energy ion scattering (MEIS) and Rutherford backscattering spectroscopy (RBS). Accurate quantification and profiling of hydrogen in thin-layer materials is challenging. The detection limit of traditional methods, such as secondary ion mass spectroscopy (SIMS) is about 10^{15} H/cm^3, which is comparable with the density of dangling bond at the non-passivated SiO_2/Si interface (1×10^{13} cm^{-2}) as measured by electron spin resonance. Here we use ERD as an alternative to SIMS for accurate quantification of hydrogen isotopes.

Medium energy ion scattering results indicate that distribution of Si, O and N are as expected from the deposition parameters. A simulation of MEIS spectra showed that the outermost layer was silicon oxinitride film with a thickness of 20 ± 2Å. The position of the nitrogen peak indicates that most of nitrogen is confined within silicon nitride layer, however there is some interdiffusion of N into SiO_2 layer at the interface. Our results indicate that with increasing silicon nitride thickness there is a significant decrease in interfacial defect density and fixed charged densities (Figure 1).

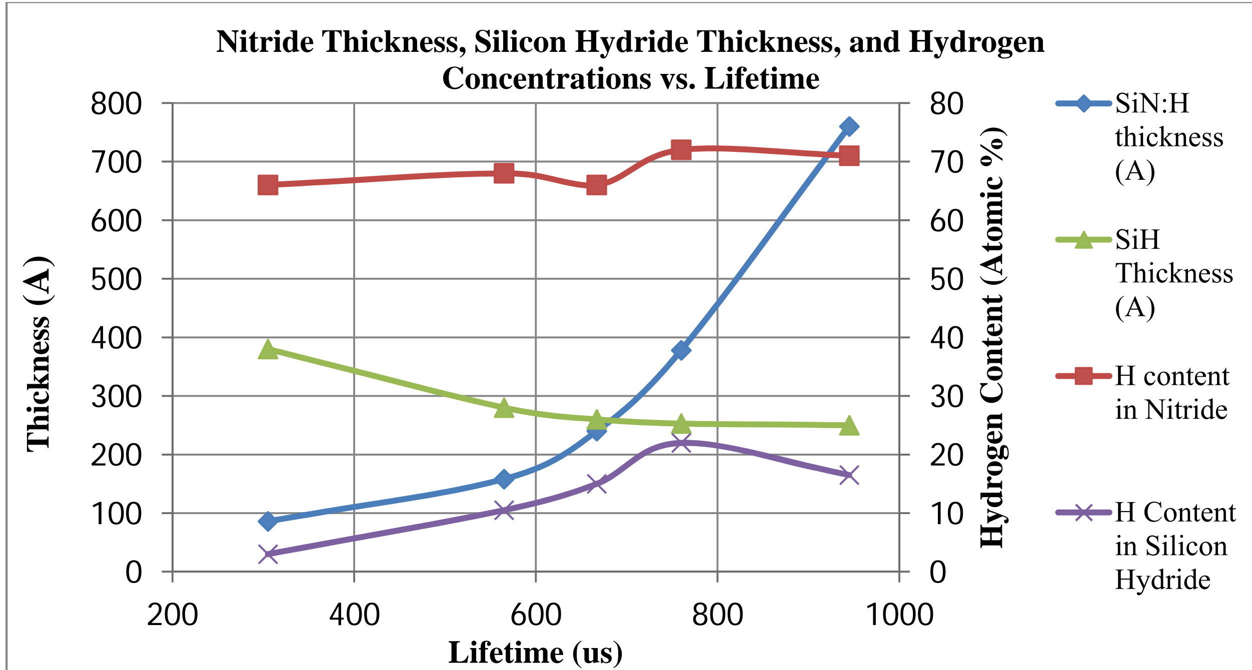

Figure 1: Silicon nitride thickness and hydrogen content variations with the observed lifetime of the solar cell devices.

There appears to be a correlation between an increased H content at the SiO_2/Si interface and higher observed minority carrier lifetimes. We argue that in the proposed passivation scheme, we achieve efficient termination of Si dangling bonds. There is no significant dissociation of Si-H bonds at temperatures below 600°C, while silicon nitride functions as a very good barrier for hydrogen diffusion. Further study of temperature related processes is needed to better understand the role such H content plays in the passivating native oxide-Si interfaces.

[1] Z. R. Chowdhury, K. V. Cho and N. P. Kherani, Applied Physics Letters **101** (2), 4 (2012).
[2] C. Krug, E. P. Gusev, E. A. Cartier and T. H. Zabel, Journal of Applied Physics **95** (3), 887-895 (2004).
[3] C. G. Van de Walle, J. Vac. Sci. Technol. A-Vac. Surf. Films **16** (3), 1767-1771 (1998).

P-2

Synthesis and characterisation of silicon nanoclusters in alumina

C.C. Cadogan[1], V.L. Karner[2], A. Tavares[1], A. Pywowarzcuk[1], P.J. Simpson[1], L.V. Goncharova[1]

ccadogan@uwo.ca

[1]*Department of Physics and Astronomy, Western University, London, ON, Canada*
[2]*Department of Chemistry, University of British Colombia, Vancouver, BC, Canada*

Si has been shown to display unique electrical and optical properties when its size is reduced to the material's Bohr exciton radius. Si nanoclusters (Si-NCs) embedded in dielectric materials have been the subject of intense research due to their potential applications in optical and optoelectronic devices. However, there is an incomplete understanding of the processes responsible for the properties of Si-NCs, particularly the mechanism by which Si-NCs luminescence.[1-3] Gaining an understanding of these processes would aid in the development of a Si-based light source, which is key to the development of high efficiency optical and optoelectronic devices. In our study, we synthesized Si-NCs embedded in Al_2O_3 and analyzed their optical properties. Al_2O_3 is used as the host medium because it has a band gap energy that is adequate for charge carrier confinement, and a high dielectric constant which makes it a promising candidate for charge storage devices.[4] In addition, the transparency of Al_2O_3 makes it suitable for the fabrication of transparent devices.

In our study, Si-NCs were produced by ion implantation of Al_2O_3 with Si ions followed by an annealing process. The amorphous Al_2O_3 films used were synthesized by anodization of Al foils, and crystalline samples were purchased from MTI Corporation and Valley Design Corporation. An in-depth analysis of the structure, composition and optical properties of these Si-NC/Al_2O_3 structures was conducted using particle induced x-ray emission (PIXE), Rutherford backscattering spectroscopy (RBS), photoluminescence (PL) spectroscopy, time-resolved PL (TRPL), cathodoluminescence (CL) spectroscopy, scanning electron microscopy (SEM), powder x-ray diffraction (XRD), Fourier transform infrared spectroscopy (FT-IR) and x-ray absorption near edge spectroscopy (XANES). From these analyses we conclude that the luminescence of Si-NC/Al_2O_3 is heavily impacted by the presence of defects sites within the matrix and Si diffusion within the matrix is negatively impacted by the crystallinity of the Al_2O_3 matrix.

References

[1] Giorgis, F., et al. *Phys. Rev. B* 61 (2000) pp 4693.
[2] Wang, M., et al. *Appl. Phys. Lett.* 90 (2007) pp 131903.
[3] Canham, L. T. *Appl. Phys. Lett.* 57 (1990) pp 1046.
[4] Yanagiya, S., et al. *Journal of Electronic Materials* 28 (1999) pp 496.

P-3

Depth profiling of silicon quantum dots formed in ion-implanted thermal oxide thin film

J.M. Gaudet, P.J. Simpson

jgaudet9@uwo.ca

Western University, Department of Physics and Astronomy, 1151 Richmond Street, London, Ontario, N6A 3K7

Quantum dots (QD) are nanoscale (1-10nm) crystals of semiconductor material that exhibit quantum confinement of excitons when formed within a matrix of dielectric. The resulting exciton energy is characteristic of the QD dimension and has a high probability of radiative recombination. This results in a "tunable" luminescent device.

The Si-QD/SiO_2 system can be formed by the subsequent annealing of thermal oxide films grown on (100) Si wafers and subjected to high (in excess of $10^{16}/cm^2$) doses of Si^+ implanted at energies up to 1 MeV. This system has numerous advantages: 1) the difference in band-gap between Si-QD and SiO_2 satisfies quantum confinement, 2) the Si-implanted/thermal oxide system has a low concentration of foreign impurities, which have an unknown or detrimental effect on QD formation and radiative recombination, 3) the fine control over implant energy and dose potentially translates into precise engineering of defect and implant concentration, and, 4) though Si and SiO_2 are immiscible, the mobility of lone Si^+ ions implanted in SiO_2 is very low. This allows for their diffusion, as well as many defect annihilation and creation processes, to be "switched" on and off by tailoring the thermal treatment of samples.

Our current understanding fails to explain the precise way in which synthesis and treatment of implanted films affects the luminescent properties. Previous work has shown [1-2] that the size of QD formed in an implanted film (as determined by high resolution transmission electron microscopy) is less strongly correlated with the concentration of implanted ions than the expected concentration of atomic vacancies caused by collision-induced atomic displacements. It is also known [3] that the thermal processing history of the material has a strong impact on QD formation and luminescent properties.

The current work expands upon this knowledge by investigating the relative abundance and spatial distribution of different defect species, as well as the depth-dependent stoichiometry and short to medium range order, of SiO_2 thin films with different Si^+ implant dose and energy. Positron Annihilation Spectroscopy is sensitive to open-volume defects, such as vacancies and voids, in thin films and has been used [4] to identify the presence of non-bridging oxygen hole centres (NBOHC) in fused silica. The slow positron beam at The University of Western Ontario allows for depth-resolved PAS with resolution as small as tens of nm. Electron spin resonance (ESR) does not allow depth resolution, but is in many ways complementary to PAS in studying thin-film defects in that it is most sensitive to paramagnetic defects and provides greater detail of defect structure. Its use [5] to measure the oxygen vacancy E' centre is widely known. By combining these techniques with structural and phase information from x-ray diffraction (XRD) and x-ray absorption near-edge spectroscopy (XANES) we gain a greater understanding of the formation of Si QD as a function of implantation and thermal treatment of thin films.

References.

[1] Size distribution of silicon nanoclusters determined by transmission electron microscopy. C.R. Mokry, P.J. Simpson and A.P. Knights. **978-1-4244-1768-1/08/$25.00©2008 IEEE**
[2] Role of vacancy-type defects in the formation of silicon nanocrystals. C.R. Mokry, P.J. Simpson and A.P. Knights. *J. Appl. Phys*. **105**, 114301 (2009).
[3] Optimized Photoluminescence of Si nanocrystals produced by ion implantation. C.R. Mokry, P.J. Simpson and A.P. Knights. *Proc. of SPIE* Vol. **6343**, 63432P, (2006)
[4] Si ion implantation-induced damage in fused silica probed by variable-energy positrons. A.P. Knights, P.J. Simpson, L.B. Allard, et. al. *J. Appl. Phys*. **79**, 12, 9022 (1996).
[5] Radiation-induced defects and electronic modification. P. Paillet, J.L. Leray and H.J. von Bardeleben (2000) in *Structure and Imperfections in Amorphous and Crystalline Silicon Dioxide*, eds R.A.B. Devine, J.-P. Duraud and E. Dooryhée, Wiley, England, p. 318.

P-4

Device for the transformation of charged particle beams using glass capillaries

A. Lagutin

and.lagutin@gmail.com

Belarusian State Academy of Telecommunications, Minsk, Republic of Belarus

Although there have been reports for transmission of ions through nano- and micro-scale single and multiple capillaries, ion transmission through tapered glass capillaries has rarely been reported so far [1]. With a length of several centimeters and a diameter of a few micrometers at the exit, these capillaries have nevertheless the same aspect ratio as the etched pores (length/diameter ≈ 100). One of the leading goals of this research on single capillaries is to produce multi-charged ion beams with diameters smaller than a micrometer (nano-beams). These glass capillaries offer the opportunity to be used as an ion funnel due to their amazing properties of guiding and focusing highly charged ion beams without altering either their initial charge state or the beam emittance ($<10^{-3}$ $\pi\cdot$mm$\cdot$mrad). However, the understanding of the underlying process is not complete and relies on models assuming charge patches distributed along the capillary and which still need to be tested.

The effect of the accumulated charge presented on figure 1, shows the time dependencies for 240 keV protons transmitted through a capillary. Competition of the processes of charging of the inner surface and charge leakage in narrow capillaries results in an oscillating time dependence of the transmitted ion current. The studied effects have allowed developing and approving the device for interruption of the ion beams on series pulse to form miscellaneous, duration, periodicity and intensities [2].

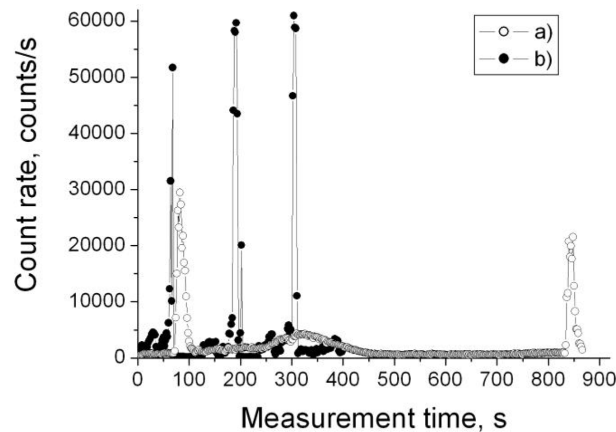

Figure 1: Time distributions of protons transmitted through a capillary with a diameter of 0.1 mm and a length of 30 mm at the axial entry angle of particles ± 0.0º. The proton current at the input of the capillary is (a) 0.85 and (b) 10 pA.

References.

[1] A. Lagutin. Proceedings of HRDP7. Singapore, 2013. http://www.hrdp7.org

[2] A. Lagutin. Abstract book of ICACS-26. P. 124-125.

P-5

PowerMEIS: RBS/MEIS simulations using cloud computing

G.G. Marmitt, H. Trombini, M.C. Sulzbach, I. Alencar and P.L. Grande

gabriel.marmitt@ufrgs.br

Instituto de Física, Universidade Federal do Rio Grande do Sul

In this work we show the integration of PowerMEIS[1] with a web server, which provides to users worldwide a platform to make and analyse RBS/MEIS simulations through any modern web browser. The web site is hosted on a server comprised of an i7 Intel Processor with 12 cores and 32Gb of DDR4 RAM. PowerMEIS parallelized algorithm handles simulations from multiple users simultaneously when needed, while it distributes a single simulation between multiple cores when idle. This platform is used for all MEIS fittings in the 2nd Round Robin Table for MEIS, and details about the employed procedure will be discussed.

References.

[1] Sortica, M. A., Grande, P. L., Machado, G. & Miotti, L. *J. Appl. Phys.* **106**, 114320 (2009).

Universal scaling of the electronic stopping cross section for swift heavy projectiles colliding with atoms and molecules

C. Martínez-Flores, L.N. Trujillo-López, L.N. Serkovic-Loli and R. Cabrera-Trujillo

cesar@fis.unam.mx

Instituto de Ciencias Físicas, Universidad Nacional Autónoma de México, Ap. Postal 48-3, Cuernavaca, Morelos 62251, México

The electronic stopping cross section and mean excitation energy for heavy ions collinding with atoms and molecules --- within the first Born approximation --- have been calculated in terms of an orbital decomposition. The harmonic oscillator approach and the virial theorem are implemented to describe the atomic target electronic structure through the mean excitation energy [1]. For molecular targets, we use the core and bonds decomposition [3]. In this work, we show that, within the Bethe theory, there is a universal scaling when the electronic stopping cross sections and projectile kinetic energy are scaled properly in terms of the target mean excitation energy for all projectile–target combinations. We provide an analytic expression for the stopping cross section that depends only in terms of the target properties [2]. Finally, we verify the universal scaling law by comparison to atomic and molecular experimental data available in the literature. The scaling rule is useful to describe the electronic stopping cross section for projectile-target systems that have not been experimentally measured yet [3].

References

[1] R. Cabrera-Trujillo, Phys. Rev. A 60 (1999) 3044.

[2] R. Cabrera-Trujillo, C. Martínez-Flores, L.N. Trujillo-López and L.N. Serkovic-Loli. Radiation Effects & Defects in Solids, 2016.

[3] L.N. Trujillo-López, C. Martínez-Flores and R. Cabrera-Trujillo. Nucl. Instrum. Methods Phys. Res. Sect. B 2013, 313, 5.

MEIS-K120 using 100 keV He^+ and TOF analyzer

W.J. Min[1], W.S. Kim[1], K. Park[1], K.H. Jung[1], S.Y. An[1], J.-s. Kim[1], S.G. Kim[1], C.S. Sim[1], S. Kim[1], J. Kim[1], K.-S. Yu[1], M.A. Sortica[2], P.L. Grande[2] and D.W. Moon[3]

dwmoon@dgist.ac.kr

[1] K-MAC, 33, Techno 8-ro, Yuseong-Gu, Daejeon 305-500, Rep. of Korea.
[2] Instituto de Física, Universidade Federal do Rio Grande do Sul, Avenida Bento Gonçalves 9500, 91501-970 Porto Alegre, Rio Grande do Sul, Brazil
[3] Department of New Biology, DGIST, Dalseong, Daegu, 711-873, Republic of Korea

Time of Flight - Medium Energy Ion Scattering spectroscopy (TOF-MEIS) using 100 keV He^+ was commercialized at K-MAC, Republic of Korea. He^+ was created by the RF plasma ion source and accelerated to 100 keV. Then, the He^+ was focused on the sample to 30 μm ~ 1 mm by 3 einzel lens system. The continuous ion beam was chopped to 350 ps pulse beam to adopt TOF analyzer. TOF analyzer detects the scattered ion energy without loss of neutralized scattered ion. At the end of the TOF tube, the large delay line detector accepts the scattered ion with enhanced efficiency. The faraday cup was installed for monitoring the incident ion current in the middle of ion optics system. As a result, the experiment by controlling the accurate count of incident ions is possible to absolute quantification. The MEIS-K120 equipment is controlled by PC, and S/W was included the control, data acquisition, and simulation tool.

By using TOF-MEIS, we measured the elemental depth profile (including hydrogen) of various nano-scale ultra thin film such as 1, 3, 5, 7 nm HfO_2 / SiO_2 / Si, (1 nm HfO_2 / 5 nm SiO_2) × 5 / Si multilayer, arsenic ultra shallow junction in Silicon substrate, and strain profile of SiO_2 / Si interface. Even thick sample such as over 100 nm $InGaZnO_x$ was analyzed with a help of Ar^+ sputtering. In addition, the 3D compositional profiling of CdSe/ZnS quantum dot and FinFET was analyzed by using TOF-MEIS and POWERMEIS simulation.

P-8

Positron Annihilation Spectroscopy with *in situ* ion implantation to investigate defects in semiconductors over a wide temperature range

J. Rideout[1], A.P. Knights[1], P.J. Simpson[2], P. Mascher[1], J.G. England[3]

rideoujl@mcmaster.ca

[1] McMaster University, Dept. of Engineering Physics, 1280 Main St. West, Hamilton, Ontario, L8S 4L8
[2] Western University, Dept. of Physics and Astronomy, 1151 Richmond Street, London, Ontario, N6A 3K7
[3] Varian Semiconductor Equipment, Silicon Systems Group, Applied Materials Inc,
35 Dory Road, Gloucester, MA 01930 USA

PAS (Positron Annihilation Spectroscopy) is a technique that can be used to study neutral or negatively charged defects in semiconductors. Positrons are accelerated by an applied voltage and implanted into a solid sample, where they thermalize. Each positron annihilates with an electron to form two 511 keV γ-ray photons, which are Doppler-broadened due to the momentum components of the positron-electron pair. Since the momentum distribution of electrons near vacancies or voids is different than in the bulk, measuring the line shape of the 511 keV annihilation peak leads to the detection of vacancy defects [1]. The mean implantation depth of the positron beam is adjusted by changing the accelerating voltage. Combined with standardized fitting routines, PAS reveals high resolution depth profiles of the vacancy concentrations in films only tens to hundreds of nanometers thick.

For the first time, we have commissioned a dual-detector PAS measurement chamber which combines *in situ* ion implantation up to 50 kV from a gas DC-coupled plasma source, as well as a temperature controlled sample stage that can achieve temperatures from 10-1000 K. This allows the evolution of defect profiles before and after ion implantation to be observed as the sample warms and is annealed. This system will eventually be located in the McMaster Intense Positron Beam Facility (MIPBF) as an addition to the McMaster Nuclear Reactor (MNR) [2].

In this work, preliminary PAS results from the system using a Na-22 positron source will be presented. These measurements include (i) a study of Ta_2O_5 films formed by implantation of Ta metal with high doses of O for resistive memory applications [3], (ii) observing the results of process parameters on As-implanted Si wafers doped via PLAD [4], and (iii) the effect of temperature on defect evolution in Ar-implanted Si.

[1] P. G. Coleman, *Positron Beams and Their Application,* (World Scientific, Singapore, 2000).
[2] https://mnr.mcmaster.ca
[3] Materials supplied by Varian Semiconductor Equipment, SSG, Applied Materials Inc.
[4] Samples supplied by J. England, Varian Semiconductor Equipment, SSG, Applied Materials Inc.

A three-dimensional analysis of Au-silica core-shell nanoparticles using medium energy ion scattering

Z. Zolnai[1], P. Petrik[1] A. Deák[1], S. Pothorszky[1], D. Zámbó[1], G. Vértesy[1], N. Nagy[1], **A.K. Rossall[2]** and J.A. van den Berg[2]

zolnai@mfa.kfki.hu

[1]Centre for Energy Research, Institute of Technical Physics and Materials Science (MFA), Konkoly-Thege M. út 29-33, H-1121 Budapest, Hungary

[2]International Institute for Accelerator Applications (IIAA), School of Computing and Engineering, University of Huddersfield, Huddersfield, HD1 3DH, UK.

The medium energy ion scattering (MEIS) facility at the IIAA Huddersfield has been used for the analysis of a monolayer of Au-silica core-shell nanoparticles deposited on Si substrate. Both spherical and rod shape particles were investigated and the spectra produced by 100 keV He^+ ions scattered through angles of 90º and 125º were compared with the results of RBS-MAST [1] simulations performed on artificial 3D model cells containing the nanoparticles. The thickness of the silica shell, the diameter of the Au spheres, and the diameter and length of the Au nano-rods were determined from best fits of the measured set of MEIS spectra.

In addition, the effect of ion irradiation on the silica shell and gold core was monitored by MEIS measurements in conjunction with RBS-MAST simulations. Ion bombardment was performed under largely different conditions, i.e., by 30 keV Ar^+, 150 keV Fe^+, or 2.8 MeV N^+ ions in the dose range of 2×10^{15} - 2×10^{16} cm^{-2}. Significant changes in the particle geometry can be observed due to ion beam-induced sputtering and recoil effects, the significance of which was estimated from full-cascade SRIM simulations.

Rutherford backscattering spectrometry (RBS), Field emission scanning electron microscopy (FESEM), and Atomic Force Microscopy (AFM) techniques have been applied as complementary characterization tools to monitor the amount of gold and surface morphology on the un-irradiated and irradiated sample areas. We show that MEIS can yield spatial information on the geometrical changes of particulate systems at the nanometre scale.

References.

[1] Z. Hajnal, E. Szilágyi, F. Pászti, G. Battistig, Nucl. Instr. and Meth. B 118 (1996) p. 617

P-10

Structural characterization of CdSe/ZnS quantum dots using Medium Energy Ion Scattering

M.A. Sortica[1], P.L. Grande [2], C. Radtke[3], L.G. Almeida[2], R. Debastiani[2], J.F. Dias[2], A. Hentz[2]

mausortica@gmail.com

[1]Uppsala University, Ångström Laboratory, Department of Physics, Ion Physics, Lägerhyddsvägen 1, Box 516, SE-751 20, Uppsala, Sweden

[2]Institute of physics, Universidade Federal do Rio Grande do Sul (IF-UFRGS), Av. Bento Gonçalves 9500, 91501-970, Porto Alegre-RS, Brazil

[3] Institute of chemistry, Universidade Federal do Rio Grande do Sul (IQ-UFRGS), Av. Bento Gonçalves 9500, 91501-970, Porto Alegre-RS, Brazil

[4]ANKA/Institute for Photon Science and Synchrotron Radiation (IPS), Karlsruhe Institute of Technology (KIT), Hermann-von-Helmholtz-Platz 1, Eggenstein-Leopoldshafen, D-76344, Germany

Compound quantum dots QDs are promising materials that can be used in many fields of the technological development, but the accurate knowledge of compositional depth profiling inside of them is still a technological challenge. Medium energy ion scattering (MEIS) is an ion beam analysis technique, capable of elemental depth profiling with subnanometric depth resolution. Recently, the MEIS technique was optimized for nanostructured materials analysis [1] and became a promising tool for structural characterization inside of QDs [2,3].

In this work [4], we use the MEIS technique to characterize a core-shell nanostructure of CdSe/ZnS. The crystal size of 5.2 nm, determined by MEIS, is in good agreement with optical measurements and TEM images. The core-shell structure is resolved by the present configuration of MEIS in contrast to the present TEM measurements. The commercial CdSe/ZnS QDs has non-stoichiometric Cd and Se concentrations. The sample selected for this work have a Cd:Se ratio of 0.69:0.31. Our investigation shows that there is Cd present on the shell and the CdSe core tends to be a stoichiometric crystal. That indicates that, despite the unbalance of material, the CdSe crystal is preserved during the industrial process which allows the control of the QDs diameters.

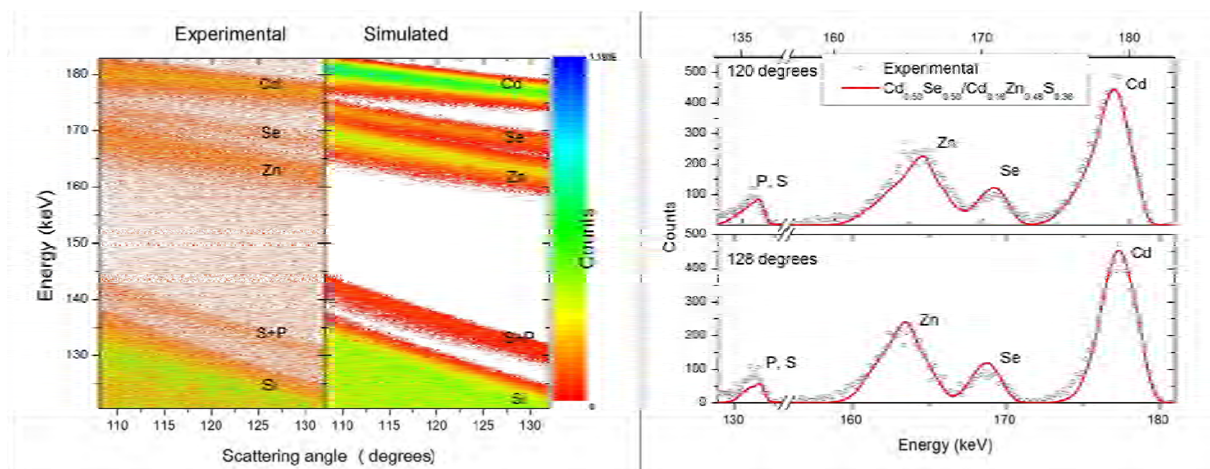

P-10

This study shows that the MEIS technique, combined with other analytical techniques, is a powerful method to determine elemental distribution profiles, inside nanoparticles with diameter about 5 nanometers. This allows studies of the formation and stability of the internal structure of QDs when exposed to several kind of processes, like heating and ion irradiation.

Keywords: MEIS, nanotechnology, IBA, perfilometry

Project financed by CNPq and PRONEX

References

[1] M. A. Sortica et al., Journal of Applied Physics 106, (2009) 1.
[2] H. Matsumoto et al., Nuclear Instruments and Methods in Physics Research B 268, (2010) 2281.
[3] J. Gustafson et al., Surface Science 605, (2011) 220.
[4] M. A. Sortica et al., Applied Physics Letters, 101, (2012) 023110.

P-11

Characterization of resistive memories using micro-beam RBS

M.C. Sulzbach, G.G. Marmitt, L.G. Pereira, P.L. Grande

milena.sulzbach@ufrgs.br

Universidade Federal do Rio Grande do Sul, Institute of Physics - Av. Bento Gonçalves, 9500, 91501-970 – Porto Alegre, Rio Grande do Sul - Brasil.

In the last years the search for new computing memory technologies has increased considerably. Different concepts of memory have been attempted to replace magnetoresistive random access memories (MRAM), the phase change and ferroelectric RAM. Recently, the resistive RAM has been investigated as possible substitute for usual MRAM [1]. Memories based on resistive switching have a capacitor-like structure composed of a semiconductor material sandwiched between two metal electrodes. This system can assume two resistance states, low and high, which is controled by the voltage bias applied over the insulator. A recent study has shown that the switching speed time can be faster than several nanoseconds [2].

For some devices, the switching phenomenon is caused by the formation of conducting metallic filaments inside the insulator. In systems where the top electrode is an electrochemical active metal and the bottom is an inert one, atoms from the top electrode move into the insulator via redox-based mechanism. This kind of system is known as Electrochemical Metallization Memories (ECM) [3]. It is also possible to observe a similar effect in systems with both electrodes being chemical inert, in which the change in resistance is attributed to the movement of oxygen vacancies inside the electrolyte.

In this work, we study devices based on TiO_2 with a platinum inert electrode and copper as active. The sample was deposited via physical vapor deposition technique (sputtering). The top copper electrode was deposited over a shadow mask to create a circular pad of 250µm diameter.

To induce the movement of copper ions into the oxide, the system requires a process called electroforming step or “soft breakdown”. In this step a certain positive voltage is applied over the copper electrode in the virgin device, which has high resistance. With the increasing voltage, the microstructure of the oxide reorganizes to create a copper conduction path. When the filament connects the electrodes, the device’s resistance has a sudden drop, as is possible to observe in the electric measurements. There is maximum current (compliance) to positive voltages to ensure the device does not break definitively.

After the device is properly on the set state, we perform the RBS micro-beam measurement, focusing the beam only over one device. Accomplishing data over virgin and setted devices, it was possible to observe evidences indicating the movement of the copper inside the TiO_2. The data were obtained with a 10µm x 16µm beam in the middle of the pad, approximately were the electrical contacts were. These results will be discussed at the conference in connection with the ones measured by MEIS after removing the copper layer by chemical etching.

References

[1] J.Yang et al., Nature Nanotechnology 8, 13–24 (2013).
[2] C.Yoshida et al., Appl. Phys. Lett. 91, 223510 (2007).
[3] L.Yang et al., Appl. Phys. Lett. 95, 013109 (2009).

P-12

Characterization of ejected CaF_2 by swift heavy ion bombardment using MEIS

H.Trombini,[1] G.G. Marmitt,[1] I. Alencar,[1] M. Hatori,[1] P.L. Grande,[1] J.F. Dias,[1]

W. Assmann,[2] M. Toulemonde,[3] and C. Trautmann[4,5]

henrique.trombini@ufrgs.br

[1]*Instituto de Física, Universidade Federal do Rio Grande do Sul, Porto Alegre-RS, Brazil*

[2]*Sektion Physik, Ludwig-Maximilians-Universät München, Garching, Germany*

[3]*Centre de Recherche sur les Ions, les Matériaux et la Photonique, Grand Accélérateur National d'Ions Lourds, Caen, France*

[4]*Materialforschung, Helmholtzzentrum für Schwerionenforschung, Darmstadt, Germany*

[5]*Fachbereich Materialwissenschaften, Technische Universität Darmstadt, Darmstadt, Germany*

Electronic sputtering effects caused by ~1 MeV u^{-1} Au ions impinging on (111) CaF_2 surfaces are investigated by the catcher technique [1]. Sputtered eject were collected on different catcher surfaces and analyzed by Medium-Energy Ion Scattering (MEIS) after an initial characterization with Transmission Electron Microscopy (TEM) and Atomic Force Microscopy (AFM). This previous characterization indicated a bimodal distribution for analyses of TEM projected images, while AFM topography showed the aggregation of spherical particles. Depending on the areal density, these nanoparticles are isolated, overlap or completely coat the catcher. Modeling such deposition with the PowerMEIS code [2] yields good agreement with MEIS spectra. By performing measurements at different collection angles for a fixed incidence angle of the primary ions, the data allow the determination of total yields as well as angular distributions. Independent of beam incidence, electronic sputtering of CaF_2 exhibits a jet-like component normal to the sample surface, as previously observed for LiF [3].

References.

[1] Electronic sputtering with swift heavy ions. W. Assmann, M. Toulemonde, C. Trautmann. *Topics Appl. Phys.* 110 (2007) 401-450.
[2] Characterization of nanoparticles through medium-energy ion scattering. M. A. Sortica, P. L. Grande, G. Machado and L. Miotti. *J. Appl. Phys.* 106 (2009) 114320.
[3] Jetlike component in sputtering of LiF induced by swift heavy ions. M. Toulemonde, W. Assmann, C. Trautmann and F. Grüner. *Phys. Rev. Lett.* 88 (2002) 057602.

P-13

3D characterization of nanostructures using MEIS

H. Trombini[1], G.G. Marmitt[1], P.L. Grande[1], I. Alencar[1] and J.G. England[2]

henrique.trombini@ufrgs.br

[1]*Instituto de Física, Universidade Federal do Rio Grande do Sul, Porto Alegre-RS, Brazil*

[2]*Varian Semiconductor Equipment, Silicon Systems Group, Applied Materials Inc, 35 Dory Road, Gloucester, MA 01930 USA*

Medium energy ion scattering (MEIS) is an ion beam characterization technique capable of determining with sub-nm depth resolution elemental composition and concentration-depth profiles in thin films [1]. This technique is widely used for analysis of microelectronic materials as well as for the determination of structural and vibrational parameters of crystalline surfaces. The former application exploits its high-energy resolution whereas the latter is achieved by measuring angular dips originated from shadowing and blocking effects[2]. More recently, the MEIS technique was used as an additional tool for the characterization of shape, composition, size distribution and stoichiometry from surface located nanoparticles (Nps) systems [3].

We demonstrate the use of MEIS for the characterization of nanostructured materials through the software PowerMeis [3]. This MEIS application is unique, and in case of elemental depth profiling in Nps, is hardly achieved by any other analytical technique. In particular it is powerful technique to characterize 3D structures as arrays of trenches and fins used to build
3D transistors. Here we investigate shallow trench isolation (STI) samples that present various trench densities obtained through chemical mechanical polishing (CMP) process.

References.

[1] Ion beam crystallography of surfaces and interfaces. J. F. Van der Veen. Surf. Sci. Rep 5, (1985) 199.

[2] Advanced ion energy loss models and its applications for subnanometric resolution elemental depth profiling using ion scattering. R. P. Pezzi, P. L. Grande, M. Copel, G. Schiwietz, C. Krug and I. J. R. Baumvol. Surf. Sci. 601 (2007) 5559.

[3] New approach for structural characterization of planar sets of nanoparticles embedded into a solid matrix. D. F. Sanchez, G. Marmitt, C. Marin, D. L. Baptista, G. M. Azevedo, P. L. Grande and P. F. P. Fichtner. Sci. Rep. 3:3414 (2013) 101038.

[4] Characterization of nanoparticles through medium-energy ion scattering. M. A. Sortica, P. L. Grande, G. Machado and L. Miotti. *J. Appl. Phys.* 106 (2009) 114320.

P-14

Quantitative considerations in medium energy ion scattering analysis of nanolayers

P.C. Zalm, P. Bailey, A.K. Rossall, and **J.A. van den Berg**

j.vandenberg@hud.ac.uk

International Institute for Accelerator Applications (IIAA), School of Computing and Engineering, University of Huddersfield, Huddersfield, HD1 3DH, UK.

Functional components in today's microelectronic devices can hardly be characterized comprehensively in situ. Increasingly, device performance prediction is based on a combination of simulations with measurements on model structures. In this context, medium energy ion scattering (MEIS) in conjunction with spectrum simulation is increasingly coming into its own, due to its unique capability of providing near quantitative compositional and layer structure information during depth profiling analysis, in favourable cases, with sub-nanometre resolution.

The attainable accuracy in MEIS depth profiling is assessed using a simple, analytical calculation on a model target system (Si with dilute impurities) and this offers an insight in what can achieved. Considering the energy difference between scattering off a surface atom and one at greater depth, a linear relationship between depth of scattering and detected energy is obtained. Although for compound materials and multilayers complications arise, a similar relationship can be shown to apply, but iterative calculations using computer simulations are then required for its demonstration. Issues associated with straggling and discrete energy losses are briefly discussed.

An analysis is then given of the yield ratio of atoms scattered off the surface and those at greater depth, concluding that this ratio follows the Rutherford inverse energy squared prediction, modified with the inverse ratio of the energies at the detector to a power ~1/2. The dependence on the energy of energy width of the detector channel or bin is determined. The effects of screening due to the non-coulombic interaction potential on the backscattering yield in MEIS which mainly affects the scattering off heavy ions, is evaluated for different energies for both H and He ions using the Andersen correction. The effect of neutralisation which is most severe for light target atoms can be less accurately predicted but a pragmatic approach employing a data set of surviving ion fractions for both H and He on various surfaces, allows its parameterization and hence the description of the convolution of these two effects. This provides the dependence both on the projectile energy and the mass of the scattering atom. Although, absolute quantification, especially when using He ions, may not always be always be achievable, relative quantification in which the sum of all species in a layer add up to 100%, generally is. This conclusion is supported by the provision of some of examples of MEIS spectra derived depth profiles of nanolayers. Relative benefits of either using H or He ions are considered.

Bulk-sensitive Hard X-ray Photoelectron Spectroscopy facility at Canadian Light Source

Q.F. Xiao[1], X.Y. Cui[1], Y.F. Hu[1] and T.K. Sham[2]

qunfeng.xiao@lightsource.ca

[1] Canadian Light Source, 44 Innovation Boulevard, S7N 0V2, Saskatoon, SK, Canada
[2] Department of Chemistry, University of Western Ontario, N6A 5B7, London, ON, Canada

A Hard X-ray Photoelectron Spectroscopy (HXPES) combined with Molecular Beam Epitaxy (MBE) system was recently commissioned at the Soft X-Ray Microcharacterization Beamline (SXRMB), a medium energy (1.7-10 KeV) beamline of Canadian Light Source. Combined with the high resolution X-ray absorption spectroscopy available at the SXRMB, high energy XPS allows for deeper penetration into a material. By controlling the incident photon energy, chemical information of the bulk and interface can be probed and the surface contamination could be avoided. It offers a powerful non-destructive technique in studying bulk and interface properties of various materials. The excellent performance of the beamline and the HXPES spectrometer is demonstrated herein using Au Fermi and 4f core lines; and the controlled probing depth of HXPES is demonstrated by tuning the photon energy (2-9 keV), in the study of a series of SiO_2/SiC multilayer samples. The electric charging effect makes the conventional XPS measurements of non-conducting samples challenging. As an application of the MBE system, to overcome the electric charging effect, the insulating SiO_2 glass was coated with a thin layer of Cr metal. Excellent HXPES results of HXPES for SiO_2 coating sample was obtained, which is compatible or better than those recorded using a Kratos spectrometer.

AUTHOR INDEX

AUTHOR INDEX

Bold face indicates **presenting authors**

Underline indicates corresponding authors

Alducin, M. 02
Alducin, M. 25
Alencar, I. 04
Alencar, I. 05
Alencar, I. 07
Alencar, I. P-5
Alencar, I. P-12
Alencar, I. P-13
Almeida, L.G. P-10
An, S.Y. P-7
Assmann, W. P-12
Avila, T.S. 06
Baddeley, C.J. 27
Bailey, P. 24
Bailey, P. 27
Bailey, P. P-14
Barchet, D. P-1
Barlow, R.J. 24
Batson, P. 13
Bauer, P. 01
Bauer, P. 02
Bauer, P. 25
Borany, J.v. 12
Borduas, G. 17
Brocklebank, M. 08
Brocklebank, M. P-1
Bruckner, B. 01
Bruckner, B. 02
Bruckner, B. 25
Cabrera-Trujillo, R. P-6
Cadogan, C.C. P-2
Chan, T.K. 26
Chatzichristos, A. 23
Chhowalla, M. 13
Chung, K.W. 20
Copel, M. 03
Corrêa, S.A. 16
Cortie, D.L. 23
Cropper, M.D. 15
Cui, X.Y. P-15
Deák, A. P-9
Debastiani, R. P-10
Désilets-Benoit, A. 17
Dias, J.F. P-10
Dias, J.F. P-12
Dosmailov, M. 25
Elliman, R.G. 09
England, J.G. 04
England, J.G. 05
England, J.G. 07
England, J.G. P-8
England, J.G. P-13

Facsko, S. 12
Feldman, L.C. 11
Feldman, L.C. 13
Fichtner, P.R.P. 06
Fujimoto, D. 23
Garfunkel, E. 13
Gaudet, J.M. P-3
Gnauck, P. 12
Goebl, D. 02
Goncharova, L.V. 08
Goncharova, L.V. P-1
Goncharova, L.V. P-2
Grande, P.L. 04
Grande, P.L. 05
Grande, P.L. 06
Grande, P.L. 07
Grande, P.L. 09
Grande, P.L. 10
Grande, P.L. P-5
Grande, P.L. P-7
Grande, P.L. P-10
Grande, P.L. P-11
Grande, P.L. P-12
Grande, P.L. P-13
Green, R.J. 18
Gustafson, J. 27
Gustafsson, T. 11
Gustafsson, T. 13
Haglund, Jr., R.F. 25
Hatori, M. P-12
Heller, R. 12
Hentz, A. 06
Hentz, A. P-10
Hirata, K. 19
Hlawacek, G. 12
Hu, Y.F. P-15
Jones, T.E. 27
Juaristi, J.I. 02
Juaristi, J.I. 25
Jung, K.H. P-7
Karner, V.L. 23
Karner, V.L. P-2
Kherani, N.P. P-1
Kiefl, R.F. 23
Kim, H.J. 20
Kim, J. P-7
Kim, J.-s. P-7
Kim, S. P-7
Kim, S.G. P-7
Kim, W.S. P-7
Kimura, K. 19
Klingner, N. 12
Knights, A.P. 29
Knights, A.P. P-8
Lagos, M. 13
Lagutin, A. P-4
Larochelle, J.-S. 17
MacFarlane, W.A. 23
Macke, S. 18
Manichev, V. 11
Manichev, V. 13
Mardare, A. 25
Marmitt, G.G. 04
Marmitt, G.G. 05

Marmitt, G.G. 07
<u>**Marmitt, G.G.**</u> 09
Marmitt, G.G. 10
<u>**Marmitt, G.G.**</u> P-5
Marmitt, G.G. P-11
Marmitt, G.G. P-12
Marmitt, G.G. P-13
Martel, E. 17
<u>**Martínez-Flores, C.**</u> P-6
Marumo, T. 19
Mascher, P. P-8
McFadden, R.M.L. 23
McGahan, Ch.L. 25
McKenzie, I. 23
Min, W.J. P-7
Mistry, S. 15
<u>**Moon, D.W.**</u> 10
<u>**Moon, D.W.**</u> 20
<u>Moon, D.W.</u> P-7
Morris, G.D. 23
<u>**Moutanabbir, O.**</u> 22
Murdoch, A. 27
Nagano, K. 19
Nagy, N. P-9
Nakajima, K. 19
Nandi, S.K. 09
Narumi, K. 19
<u>Noakes, T.C.Q.</u> 15
Noakes, T.C.Q. 27
Noël, J.J. 08
<u>**Noël, J.J.**</u> 28
<u>Osipowicz, T.</u> 26
Park, K. P-7
Pedarnig, J.D. 25
Pereira, L.G. P-11
Petrik, P. P-9
Pitthan, E. 16
Pothorszky, S. P-9
Primetzhofer, D. 02
<u>**Primetzhofer, D.**</u> 14
Primetzhofer, D. 25
Pywowarzcuk, A. P-2
Radtke, C. 16
Radtke, C. P-10
Rideout, J. 29
<u>**Rideout, J.**</u> P-8
<u>Roorda, S.</u> 17
Rossall, A.K. 04
Rossall, A.K. 05
Rossall, A.K. 07
Rossall, A.K. 15
Rossall, A.K. 24
Rossall, A.K. P-9
Rossall, A.K. P-14
Roth, D. 01
Roth, D. 02
<u>**Roth, D.**</u> 25
RRT participants 10
Saitoh, Y. 19
Sawatzky, G.A. 18
<u>**Schiettekatte, F.**</u> 21
Serkovic-Loli, L.N. P-6
Sham, T.K. P-15
Shoesmith, D.W. 28

Sim, C.S. P-7
Simpson, P.J. 29
Simpson, P.J. P-2
Simpson, P.J. P-3
Simpson, P.J. P-8
Soares, G.V. 16
Sortica, M.A. P-7
Sortica, M.A. P-10
Stedile, F.C. 16
Steinberger, R. 02
Sulzbach, M.C. P-5
Sulzbach, M.C. P-11
Tavares, A. P-2
Tok, E.S. 26
Toulemonde, M. P-12
Trant, A.G. 27
Trautmann, C. P-12
Trombini, H. 05
Trombini, H. P-5
Trombini, H. P-12
Trombini, H. P-13
Trujillo-López, L.N. P-6
Tun, Z. 28
Vajandar, S.K. 26
van den Berg, J.A. 04
van den Berg, J.A. 05
van den Berg, J.A. 07
van den Berg, J.A. 15
van den Berg, J.A. 24
van den Berg, J.A. P-9
van den Berg, J.A. P-14
Venkatachalam, D.K. 09
Vértesy, G. P-9
Vos, M. 09
Wang, H. 11
Wang, W. 26
Xiao, Q.F. P-15
Yamamoto, K. 19
Yang, J. 13
Yeo, Y.C. 26
Yu, K.-S. P-7
Zalm, P.C. P-14
Zámbó, D. P-9
Zolnai, Z. P-9

SFR MAGNIFYING NANOSCIENCE

Western

Systems for Research is pleased to support the 8th International HRDP 2016!

SFR offers the following instrumentation to facilitate quality high resolution depth profiling:

- Time of Flight SIMS
- Optical and Stylus Profilers
- FIB/Dual Beam
- Scanning Electron Microscopes

We are proud to represent these high-performance instrument manufacturers in Canada

www.sfr.ca

Western

Welcome to Western

- Bus stop
- Emergency phone
- Barrier-free (accessible) meters
- Conference parking lot
- Conference building
- Building under construction

250 Metres
Walking Time: 3-4 Minutes

THE RESEARCH PARK
London Campus
Stiller Centre
999 Collip
COLLIP CIRCLE
National Research Centre
Windermere Manor
Mogenson Building
WINDERMERE ROAD
Spencer Hall
Lambton Hall
Westminster Hall
Mount Health Centre
Ausable Hall
Bayfield Hall
Beaver Hall
Eight Level Parkade
Perth Drive Complex
Western Centre for Public Health and Family Medicine
Medway Creek
Graphic Services
Saugeen-Maitland
Siebens Lot
London Health Sciences Centre - University Campus
Chemistry Lot
Advanced Facility for Avian Research
Support Services Lot
Support Services
West Valley Building
Dental Sciences
Robarts Res. Inst.
Siebens Centre
ELGIN DR
Health Sci. Addit.
Taylor Library
Chemistry
Med. Sci. Lot
Materials Science Addit.
Visual Arts Lot
University Community Centre
Rix Clinical Skills
Medical Sci.
Bio Lab
Natural Sci.
Biotron
Biol. & Geol. Sci.
Green-houses
Kresge
HURON UNIVERSITY COLLEGE
Hellmuth Hall
Henderson House
Broughdale House
Young House
BURNLEA WALK
South Hall
O'Neill Ridley Residence
Social Science Centre
McIntosh Gallery
Collip
Labatt Visual Arts
North Campus Building
Western Science Centre
Middlesex College
Huron College Lot
Huron Dining Hall
Western Student Services
OXFORD
Stevenson Hall
Lawson Hall
Physics & Astronomy
Weldon Library
University College
Staging
MIDDLESEX
PERTH DR
RICHMOND STREET (HWY 4)
Springett Lot
Somerville House
BRESCIA UNIVERSITY COLLEGE
Ursuline Hall
Brescia Building
Weldon Lot
Law
3M Centre
Thames Hall
Arts & Humanities Building
International & Graduate Affairs Building
Delaware Hall
Medway Lot
Alumni Western Centre (BMO)
To King's University College at Western & St. Peter's Seminary
TOWER LN
EPWORTH AVE
LAMBTON DR
Talbot College
Talbot Lot
Clare Hall
Spencer Engineering
Cronyn Obs.
Alumni Hall
Heating Plant
Music Building
Elgin Hall
UNIVERSITY DR
Thames River
Richard Ivey Building
MacKay-Lassonde Pavilion
Alumni/Thompson Lot
Tennis Courts
Mother St. James Memorial Building
Wind Tunnel
Thompson Engineering
Labatt Health Sci. Bldg.
Practice Field North
SUNSET DRIVE
Sydenham Hall
Medway Hall
Alumni House
Mary Manor
WESTERN ROAD
South Valley Lot
HURON DR
Elborn College
Practice Field South
Thompson Recreation & Athletic Centre
Western Student Recreation Centre
Elgin Lot
SARNIA ROAD
PHILIP AZIZ AVE
University Child Care Centre
Ontario Hall
Essex Hall
Huron Flats Lot
Althouse Faculty of Education
Perth Hall
Althouse Lot
London Hall
TD Stadium
Platt's Lane Estates
Soccer Pitches
Alumni Field
Mustangs Field
N

© 2016. The Cartographic Section, Dept. of Geography, Western.